Energy 308 (2024) 132611

Contents lists available at ScienceDirect

Energy

journal homepage: www.elsevier.com/locate/energy

Urban energy transition: Sustainable model simulation for social house district

Andrea Vallati, Gianluigi Lo Basso, Francesco Muzi, Costanza Vittoria Fiorini *, Lorenzo Mario Pastore, Miriam Di Matteo

DIAEE Department of Astronautical, Electrical, and Energy Engineering, "Sapienza" University of Rome, Via Eudossiana 18, 00184, Rome, Italy

A R T I C L E I N F O

Handling editor: Wojciech Stanek

Keywords:
Renewable energy communities
Power-to-Heat
Decarbonization
Urban modelling Interface
Urban archetype
energy transition
Shared energy
Simulink

A B S T R A C T

Energy communities (EC) play a crucial role in driving the transition towards renewable energy sources within urban areas. This study focuses on the implementation of EC within linear mass housing in Rome, with particular attention given to the Tor Bella Monaca district. The research proposes and simulates six energy community distinct scenarios using the Urban Modelling Interface (UMI) and Simulink in order to advance understanding of this topic. These scenarios evaluate the integration of photovoltaic systems, heat pumps, and energy storage systems to determine their comprehensive effect on renewable energy production, CO_2 emission reduction, and the enhancement of self-consumption. The study findings show that higher electrification levels in an energy community lead to greater consumption of renewable energy and reduced reliance on the grid. The integration of heat pumps and energy storage further enhances energy consumption and self-sufficiency creating sustainable energy models in urban environments. With an increase in self-consumption factor and self-sufficiency factor of 0.15–0.30 and 0.11–0.13, respectively, depending on the scenario. The research highlights the importance of a thorough assessment of technology sizing and integration in order to enhance self-consumption and decrease CO_2 emissions. It proposes investigating the incorporation of both thermal and electrical storage to optimize self-consumption. Finally, the simulated scenarios underwent flexibility analyses to determine the precise energy flow capacity and the optimal setting identified through economic evaluation.

Nomenclature

ACs	Annual Costs (€/yr)
ASHP	Air Source Heat Pump
CAAC	Carbon Avoidance Annual Cost (€/tonCO_2/yr)
CAPEX	Initial Capital Expenditure (€)
CEP	Energy Vectors Purchase (€/yr)
CO&M	Operation and Maintenance Costs (€/yr)
crf	Capital recovery factor (%)
EAC	Equivalent Annual Cost
ECs	Energy Communities
Eel,DG	Electricity demand to the grid (MWh/yr)
Eel,load	Electricity overall demand (MWh/yr)
Eel,PVT	Electricity production (MWh/yr)
Eel,SC	Electricity self-consumption (MWh/yr)
Eel,SE	Electricity shared (MWh/yr)
f_{SC}	self-consumption fraction (−)
f_{SS}	self-sufficiency fraction (−)
f_{PV}	PV factor
IMPE	Imported Electricity
IRR	Internal Rate of Return
LM	Load Match index
LOLP	Loss-Of-Load Probability
NOCT	Nominal Operating Cell Temperature (°C)
PE, nREN	Primary non-renewable energy
PE, REN	Primary renewable energy
PED	Positive Energy District
PES	Non-Renewable Primary Energy Savings
PFECEL	Primary Fossil Energy Factor of National Grid
PtG	Power to Gas
PtH	Power to Heat
PtP	Power to Power
PtV	Power to Vehicles
PV	Photovoltaic
REC	Renewable Energy Community
RES	Renewable Energy Sources
sCOP	Seasonal Coefficient Of Performance (−)
SCR	Self-Consumption Ratio (−)
SPV,tot	Total PV plant surface (m^2)

(*continued on next column*)

(*continued*)

(*continued on next page*)

* Corresponding author.
E-mail address: costanzavittoria.fiorini@uniroma1.it (C.V. Fiorini).

https://doi.org/10.1016/j.energy.2024.132611
Received 17 November 2023; Received in revised form 1 July 2024; Accepted 26 July 2024
Available online 8 August 2024

(*continued*)

SSR	Self-Sufficiency Ratio (−)
TES	Thermal Energy Storage
$T_{TES,avg}$	TES water average temperature (°C)
$T_{w,sup}$	ASHP supply water temperature (°C)
$T_{w,ret}$	ASHP return water temperature (°C)
η	Efficiency

1. Introduction

The energy transition is nowadays a driving theme in the economic, social and scientific scenario [1–3] and the emphasis given to it within the European Agenda by the Sustainable Development Goals [4], specifically Goals 7 and 11, is significant of how it will lead a substantial transformation in society and urban areas in the next future. The shift from traditional to renewable energy sources (RES) is only a partial aspect of the transformation, which to be entirely realized requires a complete reconfiguration of the energy systems: the currently widespread energy model, heavily relying on centralized fossil fuel power plants, must be replaced by a new one made by numerous interconnected network of distributed systems, which operation is based on self-production of renewable energy. To realize this collective challenge it is necessary that a sharing approach is embraced instead of individual action, according to which communities must join forces [5], especially involving economically disadvantaged groups. Energy Communities (ECs) represent a way for aggregating households and enabling them to collectively generate, manage, store, and sell renewable energy locally produced; at the same time they allows the fight against energy poverty in neighborhoods, limiting energy consumption and ensuring low-cost energy supply.

The concept of energy communities was introduced in EU Legislation in 2018, through two directives part of the Clean Energy for all Europeans Package: the Directive on the Internal Electricity Market n. 944/2019 (IEM) [6] and the Renewable Energy Directive n. 2001/2018 (RED II) [1], currently being updated to RED III. In particular with the latter, which encourages the use of energy from renewable energy sources, the European Union has granted legal recognition to associations and introduced the role of renewable energy producer/consumer. The RED II Directive introduced the Joint-Acting Renewable Self-Consumers (JARSCs) and the Renewable Energy Communities (RECs) aggregation levels; the set is completed by the entities introduced by IEM, Active Customers (ACs) and Citizen Energy Communities (CECs), quite different in objectives. Italy has been particularly proactive in advancing Renewable Energy Communities from the transposition of the RED II Directive [7], implementing the latest legislative measures and continually developing new ones to create an innovative energy management model within the country [8]. The most recent development is the submission of a proposal for a decree on energy communities to promote the dissemination of self-consumption of energy from renewable resources.

ECs' topic is gaining prominence in academic research, prompting the debate around approaches, limitations, and potential they hold in the path towards the decabonization of urban districts [9–11].

Energy generation in RECs concerns both thermal and electrical production. Thermal generation fulfills heating, cooling, and hot water needs. Common technologies are boilers, heat pumps (HP), absorption chillers and cogeneration plants. However, the predominant direction in the design of EC is to electrify thermal consumption through the use of heat pumps [2]. The production of renewable electrical energy is the founding element of RECs [12]. A variety of RES can be used, however, in residential integration, photovoltaic systems (PV) represent the most widely adopted solution. The integration of fluctuating RES and the flexibility of the local energy system are ensured by energy storage technologies [2]. The most analyzed are electrochemical batteries, nevertheless such systems are often associated with high costs. In recent years the research indicates alongside Power-to-Power (PtP) ones, innovative energy storage systems such as Power-to-Heat (PtH) and Power-to-Gas (PtG) [13].

Power-to-Heat is based on the conversion of electricity into thermal energy by heat pumps, both for heating and cooling [14–16]. Compression heat pumps are commercial devices which produce heat efficiently and economically. PtH systems can be considered promising solutions for the integration of exceeding RES allowing both flexible demand and thermal energy storage (TES) [17]. Thermal storage, consisting of hot water tanks, is in fact a simple and economical solution. The potential flexibility provided by Power-to-Heat systems is related to heat pumps' and thermal storage's size, to thermal demand and to its profile [18]. Therefore, Power-to-Heat applications often have limits due to endogenous factors. The 4G district heating, a low temperature intelligent thermal grid, allows to integrate renewable generation in energy districts, decarbonizing thermal demand, reducing thermal losses and providing a cost-effective solution for the storage of intermittent generation [19]. The Power-to-Heat approach, despite its inherent constraints, is the most cost-effective to increase local electricity demand.

Conversely, the Power-to-Gas setup, while being attractive for distributed energy systems, is limited by the high costs for hydrogen production [20]. For volumetric fractions around 10 %, the existing gas infrastructure can be used for hydrogen transportation and storage [21], allowing higher self-consumption and eliminating costs of a specific supply chain. Nonetheless, due to the electrolyser's low efficiency, the savings of energy and emissions are low, making the injection of hydrogen into the gas grid cost-effective primarily for small volumetric fractions. In addition, hydrogen can be exploited for local balancing of power grids through fuel cells [22–24]. However, it is not the best option for RECs due to the low round-trip efficiency of the Power-to-Gas-to-Power process. The development of distributed generation goes together with that of Smart Grids, namely intelligent electricity grids which use information and communication technologies and are able to adapt to unforeseen fluctuations in load and production, supporting the balance between them and the quality of electricity supply [25].

Recent literature focused on strategies for the optimization of the energy communities, by integrating different generation systems and different energy carriers, individually or in combination [26].

Above all it is necessary to avoid oversizing components, which may lead to higher costs, that are economically detrimental. In this regard, literature dealing with optimal operation is widespread, compared with papers specifically regarding optimal planning of collective assets in ECs. A novel methodology for optimal planning of collective photovoltaic (PV) systems in energy communities (ECs) is introduced in Ref. [27], using multi-cut Benders' decomposition. This method is accurate, scalable, and accounts for long-term variations like degradation and inflation. A benchmark case study with six prosumers assessed the energy balance for different PV sizes. Collective PV generation significantly impacted the economy, reducing energy imports by 32 % (nearly 1200 MWh less) and increasing energy exports by 96 % as PV capacity grew from 0 to 80 kWp. Despite these improvements, imports remained higher than exports, highlighting ECs' primary focus on local demand rather than exporting surplus energy. The trend showed increasing imports due to progressive PV capacity loss from panel degradation. Exported energy showed a fluctuating pattern, influenced by both degradation and rising energy prices, which made selling excess energy more appealing. Therefore, long-term parameters like degradation and price increases present conflicting impacts on energy exports.When considering the renewable resources to be used, another criterion to take into account is resources' diversification. In Ref. [28], a case study examines the power supply of a remote isolated system using various renewable generators, diesel engines, and storage solutions. The components are sized using HOMER®, which identifies the configuration

that minimizes the net present value based on different predefined scheduling logics. The common approach, which involves identifying a primary technology supported by auxiliary systems to handle peak loads or extreme conditions, entails an inherent vulnerability of the asset: if the predominant technology experiences failures, supply problems cannot be mitigated by the auxiliary elements, which are undersized. In Ref. [29] is approached at building level a multi-objective design model of a hybrid system consisting of a photovoltaic system, wind turbines and a battery system to cover the electrical demand. The assumed objectives are minimizing the total annual cost of the system, maximizing the efficiency of the storage system, and evaluating the design effects using the Shannon-Wiener Index (SWI) and Herfindahl-Hirschman Index (HHI) for diversification and minimizing energy source concentration. This involves creating a multi-period nonlinear programming model (NLP), which addresses daily and seasonal variations in energy demand and environmental conditions, considering energy storage levels, energy trade, and grid interaction. Nonlinearities arise from the battery's state of charge and PV system efficiency. The strategy balances economic performance and energy security, with increased PV participation enhancing battery storage levels.

In [12], the study explores achieving complete self-consumption of renewable electricity in a high-capacity district of 50 users, emphasizing storage systems, polygeneration, and energy network synergies. The findings underscored the benefits of a multi-energy system but highlighted increased CO_2 emissions with storage technology due to roundtrip efficiency.

In [30], an optimized solar district heating network was integrated with a renewable-based electricity network featuring photovoltaic panels, wind turbines, and electrical storage to create a Positive Energy District (PED). Storage proved crucial for achieving zero imported electricity, reducing both imported (2 kWh/m^2/yr) and exported electricity and enhancing onsite fraction (from 1 % to 97 %).

Decision-making processes and comparative sustainability characterization of energy systems with high degrees of RES integration require well-established indicators [31,32]. In Ref. [33] a review on EnergyPLAN simulation model, proposed additional "advanced performance indicators," including the Mismatch Compensation Factor, Emission Reduction Effectiveness and Flexibility Factor. EAC was frequently chosen as representative function for technologies comparison, due to the difference among their lifetimes [34].

The study explained in Ref. [35] centers on how the transition towards renewable energy and the incorporation of digital technologies impact environmental sustainability through reduced CO_2 emissions. It highlights differences in impacts across China's eastern, central, and western regions, due to differing levels of economic development and technological integration, with pronounced benefits in the eastern areas. The research also explores nonlinear dynamics, indicating that increased digitization can sometimes exacerbate the negative impacts of energy transitions on emissions.

The study of Jradi et al. [36] analyses the improvement of energy efficiency in a residential area in Odense, Denmark, using large-scale modelling and simulation. Through the implementation of different strategies, including building retrofits, thermal comfort optimization and integration of renewable energy sources, the possibility of transforming the district into a positive energy area with surplus heat and electricity production is demonstrated. Eight different energy improvement strategies were then individually formulated, modelled and simulated. For example, adopting the Danish BR10 standard for the building envelope could reduce the total heat demand by 35 percent from 2388 to 1551 MWh/year. Another measure considered is the use of room radiators with modified set points (70/55 °C), with a 12 % reduction in heating demand. In addition, the integration of a fossil-free scenario in the district heating system could lead to a 40 % saving in thermal energy generation capacity.

However, the diversification of primary sources is generally applied to large-scale systems; in smaller systems, variability is mitigated by the introduction of storage systems.

The study in Ref. [37] explores Renewable Energy Communities (RECs) focusing on strategic placement and sizing of PV and BESS to optimize economic benefits their impact on grid stability.

A Linear Programming (LP) optimization model was developed and coupled with power flow analysis to assess the impact of various REC configurations (village, suburban, city, with 57, 144 and 555 consumers respectively), operating strategies, and battery placements. The adopted trategies include maximizing economic benefits, reducing peak grid exchange, and enhancing self-sufficiency, varying based on battery placement. Placing batteries at the feeder start, minimizes voltage deviations, reducing low-voltage grid load by up to 58 %. Optimal PV and battery capacities were notably larger in city grids to optimize economic benefits.

Guedes et al. [38] investigated various strategies for distributing collective storage and PV resources. They developed and compared fair and proportional sharing mechanisms to ensure equitable access and rights. Meanwhile, Berg et al. [39] explored the collaboration between ECs and distribution networks, emphasizing how local flexible resources enhance voltage stability.

Generally as flexible resources are considered batteries, but the achievement of electrification targets can be further facilitated through the adoption of alternative technologies for heating and cooling energy supply, therefore it is also necessary to deepen different storage systems. In Ref. [40] the optimal installation capacity of the PV system for REC with different load profiles is combined with hot water thank. To match various customers type bring higher cost saving potential.

Indeed, the concept of energy sharing is based on transforming energy consumers into prosumers, whose excess energy production can be shared with other members of the energy community; that way energy sharing between neighboring prosumers, indicated as peer-to-peer (P2P), leads to overcome the conventional peer-to-grid (P2G) trading.

Mixture of participants enhances energy sharing mechanisms by differentiating the loads.

Exploiting large areas for the installation of RES-based plants at large industrial parks, as a support for dense and energy-intensive urban areas as urban centers would maximize the benefits related to load complementarity. Similarly buildings or complexes that have geometries that make it easy to install even large quantities of PV can be a useful support to neighboring agglomerations. So far, however, the literature presents few examples of REC and PED applied to existing districts, while it is more common to find the study of new projects.

The study in Ref. [41] explores the optimal renewable energy configurations for supplying an existing district in Benevento, Italy, targeting a Positive Energy District (PED) condition. This district includes both residential and non-residential users, with real electric load profiles. The modeling tools used were TRNSYS 18, HOMER Pro®, and MATLAB. Renewable energy sources include evacuated tube collectors, PV plants, and wind turbines, with an electrolyser producing green hydrogen mixed with natural gas for domestic boilers. Four main configurations of renewable plants were analyzed, along with two additional configurations to improve self-consumption and reduce surplus energy export. The optimal setup featured south-oriented PV panels with 384 kW peak power, yielding surplus renewable thermal and electric energy supplies of 154 MWh/year and 1307 MWh/year, respectively. This setup met the users' total energy demands and achieved carbon neutrality with a Carbon Neutrality Check of 0.23, one of the novel indicators introduced for energy and environmental analysis.

Diverse energy communities (ECs) in Europe were examined in Ref. [39], focusing on member configurations, technology integration, demographics, and geographical factors. Using an optimization model, it simulates one-year operations of ECs in Norway and Spain across residential, commercial, and mixed loads. Grid impact is assessed through maximum import/export dynamics. Sensitivity analysis on PV sizing emphasizes aggregated community impact, neglecting internal distribution. Battery systems and load shifting strategies are considered.

Commercial and mixed loads show better grid compatibility in Norway and Spain respectively, whereas residential loads require larger batteries due to low load-PV correlation. Findings favor load shifting economically over battery storage. The study critiques synthetic data and short-term simulations (e.g., daily/weekly) for countries with seasonal electricity demand variations, advocating long-term data for accurate EC impact assessment.

A way for maximizing EC profitability is the variation of prosumers and consumers ratio.

The study in Ref. [42] analyzes energy generation and consumption patterns in a real energy community in Spain over one year, utilizing data from a 40.48 kWp community. The system integrates an energy storage system with a photovoltaic installation controlled by a bespoke system. Discharge timing is optimized to coincide with peak energy cost periods for enhanced energy and economic efficiency. The community consists of three consumer profiles with annual consumptions of 1500, 2000, and 2500 kWh, respectively, distributed as 15 %, 35 %, and 50 %. Without batteries, the self-consumption ratio ranges from 56 % to 76 %, with surplus ranging from 44 % to 24 %, depending on the consumer profile. Introducing batteries reduces surplus by over 65 %, with greater reductions as the number of consumers increases. The study suggests storage capacity should ideally support an average annual capacity of 23 %.

The same P2P concept extended to the neighborhood can be applied to the same residential complex when it reaches significant sizes, as often seen in post-World War II social housing complexes.

In many cases, sharing optimization focuses only on the operation phase, neglecting investment costs, which prevents a comprehensive economic view.

In [43] examines the optimal sharing of solar PV, wind power, and battery storage in a residential context, with the additional limit of a scarce time resolution, of just 24 h.

Taking up the previously mentioned topic of scheduling logics, the prospects of energy-based microgrids are closely dependent on optimization models for energy management, which based on provisions aimed at the mitigation of uncertainties'impact and trading effectiveness.

Long et al. [44] have explored the concept of energy sharing among various producers of Distributed Energy Resources within a community microgrid that incorporates PV and battery systems. Small-scale aggregate battery control based on EC requirements significantly reduced the amount of electricity fed back into the grid: when about 40 % of customers have their own photovoltaic (PV) systems, P2P energy sharing can lower the community's energy expenses by 30 % compared to P2G trading.

[45] developed an optimization model based on cost minimization for an existing REC in Austria.The REC consists of nine participants, residential and tertiary "nodes", located in the same low voltage distribution network. The total annual consumption of the whole REC is approximately 63,902 kWh/a with an hourly peak load of 18.32 kWp aggregating the individual electricity consumptions to a total load. Inoltre alcuni partecipanti già hanno PV installato, per un total amount of 25 kWp. Enabling renewable energy transfer within the REC boosts PV own use from 26.5 % to 65.2 %, reduces annual energy costs by 8.73 %, and cuts CO_2 emissions by 14.7 %.

From the above references it emerges that, due to the fact the fluctuations in renewable energy sources like solar PV can influence energy sharing among microgrid participants at various times throughout the year, it is essential to make assessments on an annual basis.

[46] introduces a data-driven dual time-scale energy management framework to address PV and load demand uncertainties, utilizing collapsed Gibbs sampling and MPC rolling optimization. The model offers lower operating costs and greater robustness than traditional methods, enhancing operational stability and providing strategies for developing energy communities. To this aim highlights how, along with timely monitoring of energy supply and demand, to own historical data is fundamental to obtain true and accurate probability distributions for system optimization and for making swift adjustments.

The transition from traditional heating systems to Integrated Energy Systems is a global trend that is receiving increasing support from governments and industries alike. The European Union's Fifth Framework Programme (FP5) and Seventh Framework Programme (FP7) have both conducted studies on the management models for IES. Lin et al. [47] explored the shift from conventional urban centralized heating systems to smart integrated energy systems. Their study highlights the crucial role of cyber-physical systems in improving the functionality and efficiency of these systems. It also addresses the challenges involved, such as the need for precise control of devices and overall system management. The coordination of multiple heating sources with varied characteristics, the delay in system response due to thermal inertia, and the effects of the heating network's topological structures are the primary complexities that need careful management.

For many years a central theme in energy research field is the building archetype, useful for BEM applications and scalability of the related results. These aspects make it a promising concept, if extended, even for the definition of Urban Building Energy Models (UBEMs), but to date it is still a major contributor to inaccuracies in UBEMs [48,49]. The importance of incorporating realistic occupancy profiles in the archetype, instead of fixed occupancy schedules, for accurate energy predictions is highlighted in Ref. [50]. Using data from the Time Use Survey, the study introduces a novel approach, leading to 8%–10 % variations in annual energy demand across different spatial scales in residential building archetypes. In an effort to bridge the information deficit related to the assessment of occupants' influence on energy outcomes within UBEMs across various spatial and temporal scales, Causone et al. [51] introduced the utilization of smart meter data and a method for incorporating data-driven schedules into UBEMs.

The experimental measurements indoor air parameters have been performed [52] in a selected room and values of temperature, relative humidity and CO_2 concentration have been recorded. Also, people involved in this investigation have made their own evaluation. They, have been asked for opinion about the internal air quality at the beginning and at the end of the experimental measurement.

In the end, although many studies have focused on the optimization of the PV size for RES integration in buildings, and literature concerning PtH in distributed energy neighborhoods is on the rise, to the best of the authors' knowledge the topic of energy transition applied to high density building still shows gaps. In this context, the definition of an urban archetype has the potential to be a valuable tool to manage self-consumption's maximization. In this circumstance, having observed that the widespread approach in REC modelling is to size the PV plant based on the maximum electrical requirement [53–55], to highlight how the oversizing of the plant does not mean improvement of self-consumption, and how self-consumption and self-sufficiency are related to the size of the plant is considered noteworthy. Multi-objective problem formulation, taking into account environmental and economic aspects, is a main aspect of the proposed methodology, due to the importance of holistic vision from the investors point of view.

In the present work an urban area in Rome dedicated to social housing was the object of the study, to facilitate its transition to an EC. Specifically it is Tor Bella Monaca, within the R5 District. The main reason for choosing the building typology which shapes the entire neighborhood, is the energy inefficiency, caused in particular by problems with the building envelope [56,57]. The haste in construction that characterized the mass housing developments between the 1950s and 1980s, period in which falls the realization of Tor Bella Monaca, often led to weaknesses in the durability of building materials. In fact, in the post-World War II period, the rapid increase in the demand for housing, mainly driven by the growth of population and the people migration from rural areas to urban centers, led to an impetuous development. The buildings' construction followed a modern planning paradigm, based on standardized and fast construction methods, with the aim of creating experimental self-sufficient urban communities of high density

buildings, which would integrate all the necessary services for residents. These housing projects, prevalent in the European suburbs, have often been designated for social housing. Moreover, in Rome, approximately 400,000 people currently reside in low-cost social housing projects constructed during the same time period as the studied one. This offers a compelling reason to investigate Energy Communities applied to social housing, specifically in linear multi-story buildings, which constitute a significant portion of the stock for this intended use.

Based on the potential of ECs to offer an innovative solution for managing renewable energy produced at local level, the present study aims to evaluate the impact of integrating PV, HP, and TES in energy communities, on self-consumption, non-renewable primary energy need and CO_2 reduction.

The first activity of the present study was to set up an archetype of post war linear residential buildings, selecting constructive and energy data collected from documents and on-site investigations. The results were used to recreate a 3D model of the neighborhood, then the energy consumptions were estimated using a UBEM [58] tool, namely Urban Modeling Interface (UMI) [59]. Data exported from this phase were implemented in Simulink to develop semi-dynamic energy simulations.

First of all a parametric analysis was carried out, which concerned the variation of four different parameters: the installed power of the photovoltaic field, up to the maximum installable for access to incentives of 1 MW, the degree of electrification of thermal consumption, and the prosumer and consumer distribution. The analysis was conducted in terms of energy shared by the REC (fsh), self-sufficiency fraction (fss) and self-consumption fraction (fsc).

After that, six scenarios with increasing technological integration were compared and commented. For each of the six scenarios, along with individual users' energy demand, the models incorporated variables including solar energy production and energy fed back into the grid. Scenarios from the first to the third simulated the integration with photovoltaics with a capacity equal to 100 % of the energy needs, the installation of a heat pump powered by the photovoltaic system, and the further incorporation of a thermal storage respectively. In the remaining, from the fourth to the sixth, the technological enhancement followed the same path but the capacity of the photovoltaic system was reduced to 50 %.

1.1. Building archetype

The TBM district in Rome is a prime example of the fundamental features of Italian mass housing built from the 1960s to the 1980s within the PEEP (low-cost social housing schemes) and Law 167/62.

The TBM megastructure spans around 2,500,000 cubic meters and was originally designed to house roughly 27,000 inhabitants. The residential area embodies the typical characteristics of numerous high-density housing neighborhoods in Italy and adheres to the planning ideals implemented in Europe during that era [56]. This study focuses on the monumental in-line-multistorey building R5 (Fig. 1).

The development of a specific building archetype for public housing was made possible by the study of Vallati et al. [60]. Once the specific building type was identified, an important step was to collect data from several buildings of the same type to develop an archetype. This involved a comprehensive collection of data on various aspects, including construction systems, building materials, energy consumption, and occupancy.

In the present research, a specific methodological procedure was applied to delineate the archetype of linear residential buildings constructed in the post-war period. These data were then subjected to statistical analysis to identify patterns and relationships between key variables and factors influencing the design of the archetype. An example of analysis was the use of regression to determine the relationship between building size and energy consumption.

Cluster analysis was used to group buildings by construction materials or design characteristics. In this archetype, the major components were analyzed to statistically evaluate the most recurring characteristics, following established methods in archetype construction. Data collection included architectural and urban design aspects such as building height, number of floors, total floor area, and use, obtained through site visits and review of relevant documentation. On site global heat transfer measurement through a TESTO 635-2 heat flow meter). Therefore, the wall heat transfer of 38 apartments were measured on site and the average value was used to match the wall transmittance of the archetype and thus in the Energy Model (Fig. 2).

Energy data was collected through on-site measurements, analysis of energy bills, and assessment of building mechanical systems, including data on energy sources and total energy consumption. It is important to note that due to practical limitations it was not possible to collect all available data, but only four representative dwelling type in respective

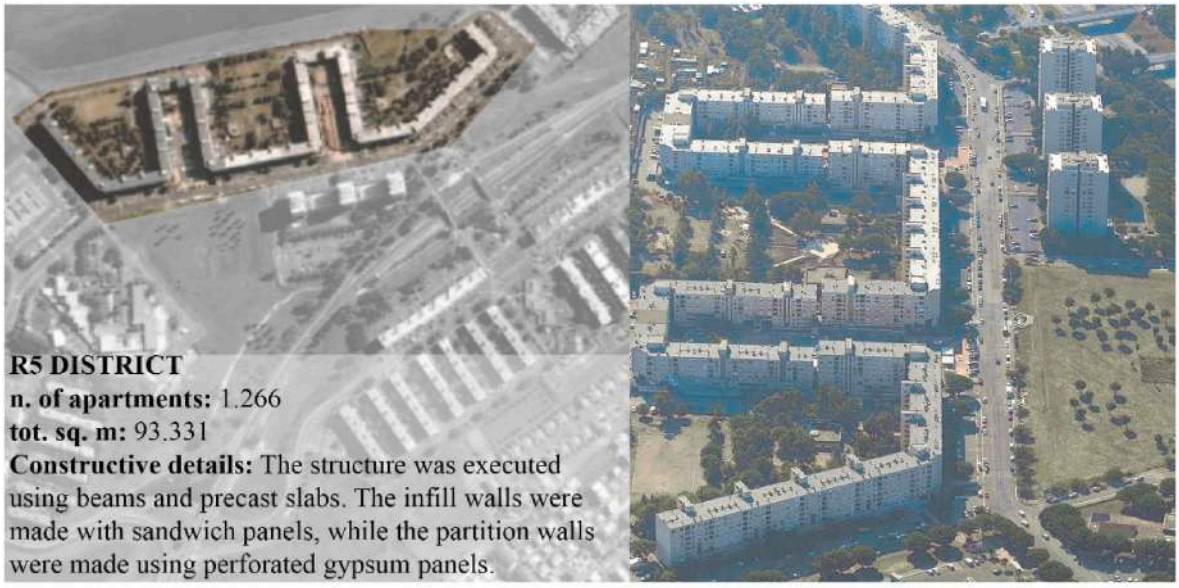

Fig. 1. R5 district.

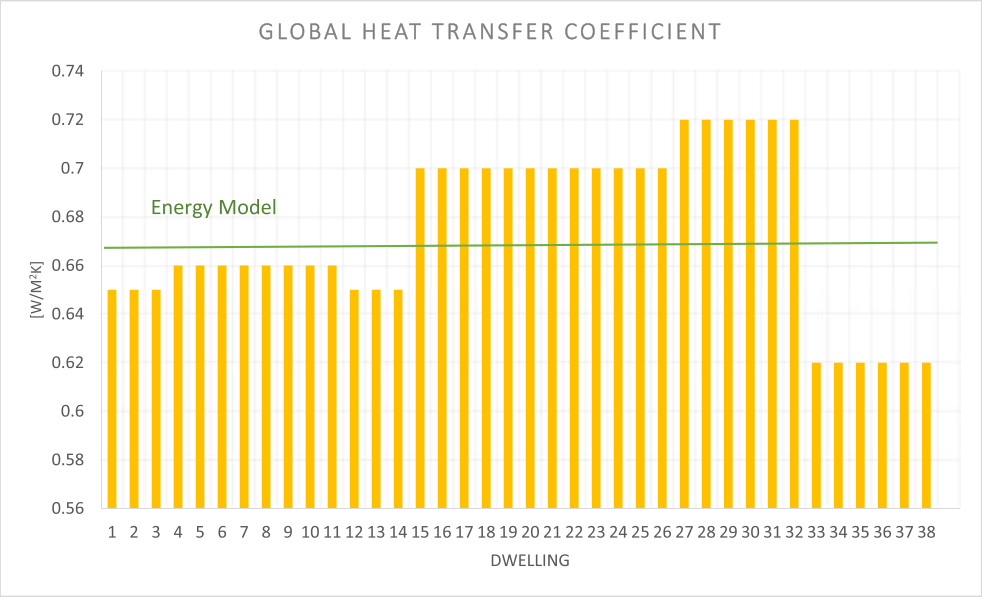

Fig. 2. Global heat transfer analysis.

four transect was included in the analyses (Fig. 3).

The results obtained make it possible to identify trends, define performance benchmarks, and contribute to the formulation of policy decisions on energy efficiency and sustainable urban development. However, the results obtained indicate that the archetype, once developed, was compared to the Tabula model. This comparison showed that the Archetype was more energy efficient, as it was able to maintain a lower annual energy consumption than the TABULA model [61]. This positive result can be attributed to the differences in the management of energy consumption and the technological characteristics of the systems used in the archetype.

This data was then processed by a Geographic Information System (GIS) [62]. Initially, spatial data, comprising floor plans of edifices, roads, parks, and the adjacent urban development, was amassed. Subsequently, the shapefile data underwent processing using Grasshopper scripts [63], which can link a reference layer to each category.

The polygon was created by converting the shape-point into a polygon. After setting the heights, Rhinoceros processed the polygon for extrusion, producing the 3D building model. In addition, Grasshopper scripts were used to transform GIS plans into 3D models of the buildings using the Rhinoceros environment [59] and a building template was assigned to each buildings model created.

Archetype proposes a new approach to the creation of archetypes that goes beyond the technical and architectural characteristics of buildings, placing a strong emphasis on energy aspects.

By analyzing real data, such as hours of heating use, it has been possible to create a comprehensive model for various public residential buildings in Italy and Europe. UMI simulated all the energy consumption of the buildings studied. The data export mechanism was configured to provide hourly consumption for each load type (e.g. electricity, heating) for individual buildings and for the entire urban area.

2. Materials and methods

This section details the methodology (Fig. 4) employed to characterize the considered scenarios. The energy model is subsequently described, along with the Key Performance Indicators (KPIs) considered.

The article is structured on three different macro-sections. The first, already addressed in the previous sections, sees the characterisation of the building archetype and its validation, while in the next two macro-sections we move on to the analysis of the renewable energy community (REC). Specifically, in the second macro-section, a parametric analysis is developed that correlates the installed photovoltaic capacity, the degree of electrification of consumption, the distribution of prosumers and consumers within the REC itself, the inclusion of thermal-electric storage tanks, and different operating strategies to the variation of shared

Fig. 3. Graphic representation of transects.

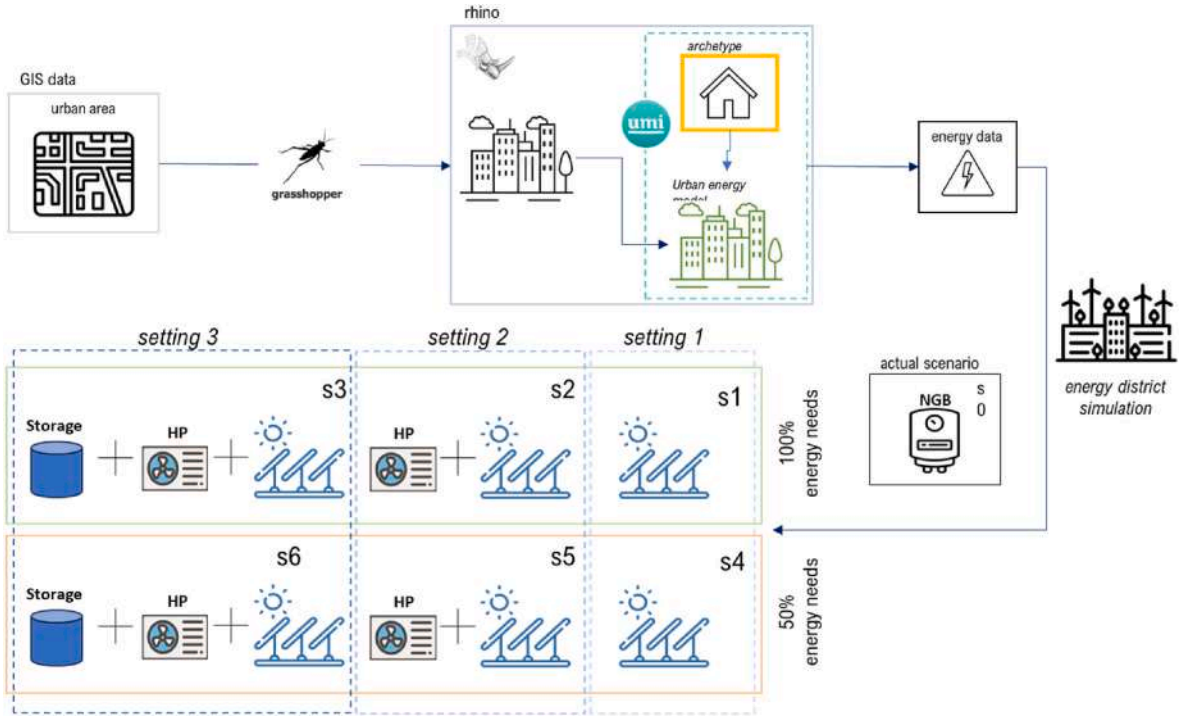

Fig. 4. Digital methodology workflow.

energy in the REC. The last macro-section sees the detailed analysis of some specific case histories, detailed in more detail below.

2.1. Parametric analysis

This section will further describe the parametric analysis of the second macro-section previously announced.

Given the thermal and electrical loads of the building and its orientation and geographical location, the parametric analysis involved the variation of four different parameters. As a first analysis, the installed power of the photovoltaic field was varied from a minimum of 10 kW, with an increment of 10 kW, up to the maximum installable for access to incentives [27] equal to 1 MW. The degree of electrification of thermal consumption was then varied from 0, production of heat from fossil or non-electric sources only, to 1, total production of heat from electric energy, with a gradual increase of 10 %. Next, 10 different scenarios were considered in order to analyze the energy dynamics within the REC by considering differently the share of consumers and prosumers constituting the energy community itself. This was done by considering a dedicated POD (Point of Delivery) in the base scenario and a prosumer share (Pdg) equal to 0, up to considering the entire prosumer user itself (Pdg = 1). Different thermal reservoirs were then sized using two different approaches, the first according to the maximum thermal load to be electrified and thus the degree of electrification, and the second according to the maximum electrical production and thus the installed photovoltaic power.

For the purpose of the analysis, the fraction of energy shared by the REC (fsh), the fraction of self-supply (fss) and the fraction of self-consumption (fsc) were taken into account as KPIs. Defining respectively fsh as the ratio between the energy produced by the PVs and absorbed/consumed within the ERC itself and the entire annual photovoltaic production, while fsc as the ratio between the energy produced and self-consumed by the prosumer and the annual photovoltaic production, finally, fss as the ratio between all the energy produced by the PVs and consumed within the ERC perimeter (both by prosumers and consumers) and the annual electricity demand of the ERC.

2.1.1. Thermal storage dimensions

Two different approaches were analyzed for the dimensioning of thermal storage, the first based on the maximum excess electrical energy on the day of greatest production, and the second based on the maximum thermal demand to be satisfied. Both approaches aim to estimate the energy to be stored in the storage, and from there the volume.

In the first approach, the focus is on maximum production and the objective of maximizing the use of electricity from internal production at the REC. To this end, the day of maximum production, the peak day, was identified, the electrical energy produced and the electrical energy required on the same day was evaluated, and above all, the electrical energy in excess of the ERC's requirements was calculated. As mentioned, the objective in this approach is to size the storage according to power to heat and to convert and store all the electrical energy produced into thermal energy by setting the energy to be stored equal to the previously calculated surplus. Given this approach, the volume will be a function of both the installed photovoltaic capacity and the degree of electrification, while the total HP power is set equal to the maximum heat demand.

The second approach instead focuses on heat demand. Placing itself on the day of maximum thermal demand and imposing continuous operation of the HP, the overall power of the HP is first evaluated, which will be less than the maximum load of the building and such that the energy not covered directly by the HP itself will be satisfied by the thermal energy accumulated in the storage during the operation of the HP at times of lower load or no load. Therefore, the power is evaluated in such a way that the energy to be covered by the storage is equal to the excess energy produced by the HP. Given the dimensioning principle of the storage and HP, these two will be a function of the load and thus the degree of electrification, but not the capacity of the PV array.

A graphical representation of the volumes and overall HP power as a function of the above-mentioned quantities can be found in the results section.

2.1.2. Notes on heat pump dimensioning

Previously, the criterion by which the maximum HP power is selected to meet the heat load of the REC was described. This section

goes into more detail on this subject. Specifically, once the maximum load to be covered has been defined, this can be satisfied by several heat pumps working in cascade according to actual demand. It is therefore necessary to define the size of the individual machines and therefore the number of machines installed.

Taking classic commercial heat pumps into consideration, six different sizes were selected and a nominal heat capacity (Pth,HP,nom) and a nominal COP (COP) were associated with each of them (Fig. 5). Having fixed the minimum modulation capacity at 15 %, the minimum power that the individual machine can deliver was calculated.

The six sizes were selected such that, knowing the maximum load required, the number of machines would be adequately distributed over the 7 blocks that make up the building.

Know a certain load to follow, the smaller the size of the HP the more I can go down to smaller loads, a 70 kW size HP with a cf 0.15 can modulate up to 10.4 kW, while smaller sizes such as the 22 kW with a cf 0.15 can reach a minimum deliverable power of 3.3 kW, going to better follow the load.

Furthermore, in order to utilise power to heat to store excess electrical energy in the form of heat, the total installed size of the HP and individual machines must be related to the electrical excess to be stored. The upper limit corresponding to the maximum power installed by the HP remains a function of the heat requirement and thus the degree of electrification. In fact, if more power were to be installed than the thermal load, it would be possible to store more electrical energy in the form of heat, but there would not be enough thermal load to empty the reservoirs and allow thermal-electrical energy to be stored again.

2.2. Scenarios characterization

In section 2.2, the last macro-section announced at the beginning of the chapter is introduced. Specifically, six specific cases are analyzed, divided into two groups, each with three different settings. The first of the three settings has a degree of electrification equal to 0, the second has a degree of electrification equal to 1 without storage, and finally the third has a system similar to the previous one, but with thermal storage.

The two groups are defined on the basis of the photovoltaic fraction (f_{PV}) defined as the ratio between the installed capacity of the photovoltaic array and the electrical power required in the absence of electrification of consumption. The first group will have an f_{PV} of 1 and the second of 0.5 (Fig. 6).

The simulated scenarios are described in detail below.

- Scenario 1 (s1): This scenario assesses the trend in self-consumption when only roof-mounted photovoltaic systems are installed ($f_{PV} = 1$). The focus is on understanding the impact of photovoltaics on self-consumption, which refers to the consumption of generated solar energy directly within the building;
- Scenario 2 (s2): In this scenario, the study evaluates the changes in energy self-consumption by integrating photovoltaic systems ($f_{PV} = 1$) with a heat pump system for heating and hot water. The aim is to analyze the combined effect of solar electricity generation and heat pump technology on self-consumption;
- Scenario 3 (s3): The third scenario models the trend towards greater energy self-consumption through the incorporation of thermal storage in s3;
- Scenario 4 (s4): Similar to Scenario 1, this scenario examines the trend in self-consumption, but with the installation of roof-mounted photovoltaic systems ($f_{PV} = 0.5$) only;
- Scenario 5 (s5): This scenario investigates the impact of integrating photovoltaic systems ($_{PV} = 0.5$) with a heat pump system on self-consumption, similar to Scenario 2;
- Scenario 6 (s6): Similar to Scenario 3, but the incorporation of thermal storage is applied on s5.

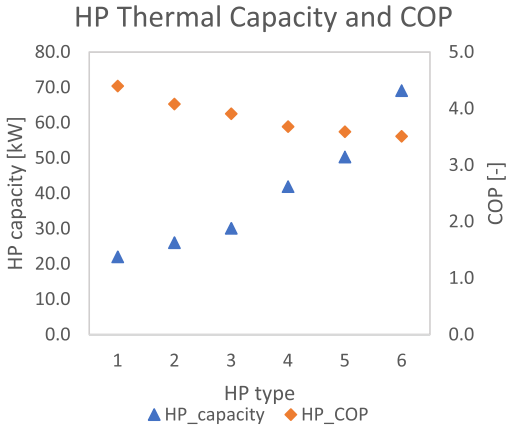

Fig. 5. Single HP nominal thermal capacity and nominal COP.

In Table 1 the technical assumptions used for the dynamic simulations are summarized.

The PV, HP and TES capacities have a significant impact on the results. In this regard, two different PV panel capacities 393 kWp in scenarios s1, s2 and s3 and 197 kWp in scenarios s4, s5 and s6 were considered. The HP capacity was selected based on the thermal load of the archetype, thus evaluating the results with respect to the presence or absence of the centralized HP system.

While for the TES, a sensitivity analysis was performed to account for the variation in results as the TES volume itself changed as reported in section 3.2. Accordingly, a volume with adequate capacity for the system was assumed, and the effect of including or not including it for different sizes of PV was compared.

The purpose of these scenarios is to analyze the potential benefits and trends in self-consumption when utilizing renewable energy systems. By assessing the different settings and scenarios, the study aims to provide insights into the feasibility and effectiveness of incorporating renewable energy technologies for meeting energy demand, both with and without the integration of heat pump systems.

In addition, the simulations between the different scenarios were compared to see which setting provides the highest percentage of self-consumption in relation to energy efficiency. A further comparison can be made between the avoided greenhouse gas emissions.

Therefore, s2, s4 scenarios use electricity as the energy carrier to power heating and domestic hot water; in contrast, the s1, s3 scenarios use natural gas to meet these loads. In fact, scenarios 2 and 4 have a higher energy demand (Fig. 7 a) due to the use of the heat pumps. While the scenarios s3 and s6 in addition to presenting the same load of the two previously mentioned are integrated with a thermal storage system increasing the matching between production and consumption. On the other hand, electricity production from solar energy is twice as high in the configuration where the photovoltaic system is sized at 100 % of the building complex's energy needs (s1, s3) for a total of 1.7 GWh/y compared to the second configuration with 50 % sizing, which has 0.85 GWh/y (Fig. 7 b).

2.3. Energy model

Energy systems were dynamically implemented in the MATLAB-Simulink environment and simulated on an hourly basis for an entire year. Specifically, the balance equations governing energy flows, as described in Fig. 8, were implemented, and a model was constructed for each energy scenario.

The time-dependent energy balance equations are as follows:

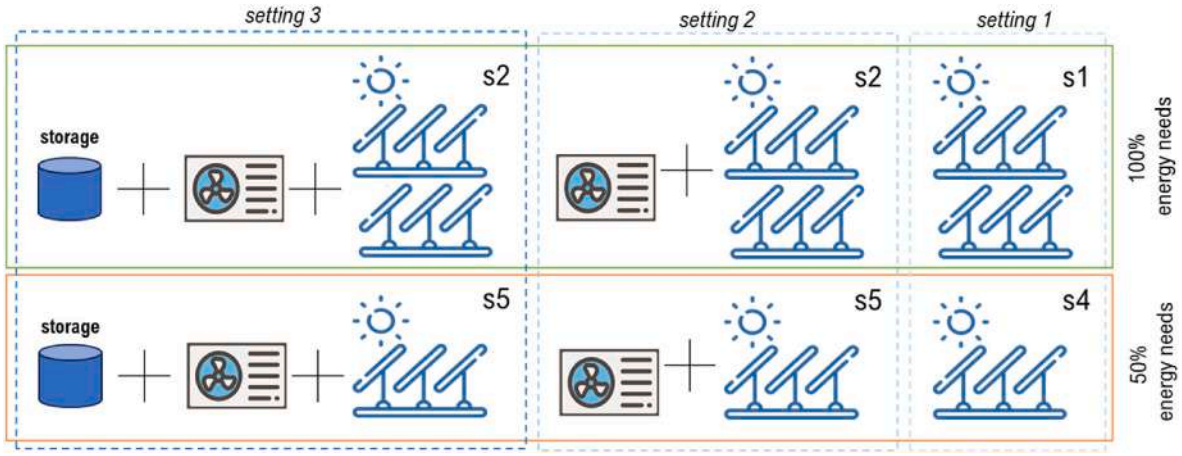

Fig. 6. Graphic representation of simulated scenarios.

Table 1
Technical assumptions for simulations.

Component	Parameters				
PV100	Power [kWp]	η	NOCT [°C]	SPV,tot [m^2]	n elements
(f_{PV} = 1)	393	0.18	43.6	4762	2381
PV50	Power [kWp]	η	NOCT [°C]	SPV,tot [m^2]	n elements
(f_{PV} = 0.5)	197	0.18	43.6	2381	1190
ASHP	Thermal capacity [kW]	sCOP	$T_{w,sup}$ [°C]	$T_{w,ret}$ [°C]	n elements
	804	3.8	55	50	12
TES	Total volume [m^3]	$T_{TES,avg}$ [°C]			n elements
	200	44 ± 2			12

$$\dot{E}_{el,load}(t) - \dot{E}_{el,PV}(t) \begin{cases} if > 0\ then = \dot{E}_{el,demand}(t) \\ if < 0\ then = \dot{E}_{el,exces}(t) \\ if = 0\ then = 0 \end{cases} \quad (1)$$

If there is no energy storage system, the energy flows can be defined as follows:

$$\dot{E}_{el,demand}(t) = \dot{E}_{el,grid}(t) \quad (2)$$

$$\dot{E}_{el,excess}(t) = \dot{E}_{el,inj}(t) \quad (3)$$

Where $\dot{E}_{el,grid}(t)$ is the energy offtake from the grid and $\dot{E}_{el,inj}(t)$ is the energy injected into the grid.

In this case, without energy storage, the self-consumption energy ($\dot{E}_{el,sc}(t)$) is given by (Fig. 8 a):

$$\dot{E}_{el,sc}(t) = \left(\dot{E}_{el,load}(t) - \dot{E}_{el,demand}(t)\right) + \left(\dot{E}_{el,PV}(t) - \dot{E}_{el,exces}(t)\right) \quad (4)$$

In the absence of thermal storage $\dot{E}_{el,load}(t)$ represents the entire electrical demand, encompassing both power and the electrical load associated with heating production for heating, cooling, and DHW. When an energy storage system is present, the balance equations of the Power-to-Heat (PtH) system are formulated by initially considering $\dot{E}_{el,load}(t)$ as solely the electrical power demand, defined as follows: If there is an energy demand ($\dot{E}_{el,load}(t) - \dot{E}_{el,PV}(t) > 0$) then the system take the required electricity from the grid. In the case of Renewable Energy Source (RES) excess ($\dot{E}_{el,load}(t) - \dot{E}_{el,PV}(t) < 0$) this surplus energy is converted into thermal energy, constrained by the Heat Pump's (HP) capacity, and compared with the thermal load ($\dot{E}_{th,load}(t)$) as illustrated in Fig. 8 b.

If there is excess of thermal energy ($\dot{E}_{el,excess}(t) * COP - \dot{E}_{th,load}(t) > 0$)) then the energy flows can be defined as follows in order to account for the TES' limitations on the state of charge:

$$MIN\left[\dot{E}_{th,exces}(t), \dot{E}_{th,available\ charge,t}(t), P_{max,TES}\right] = \dot{E}_{th,st}(t) \quad (5)$$

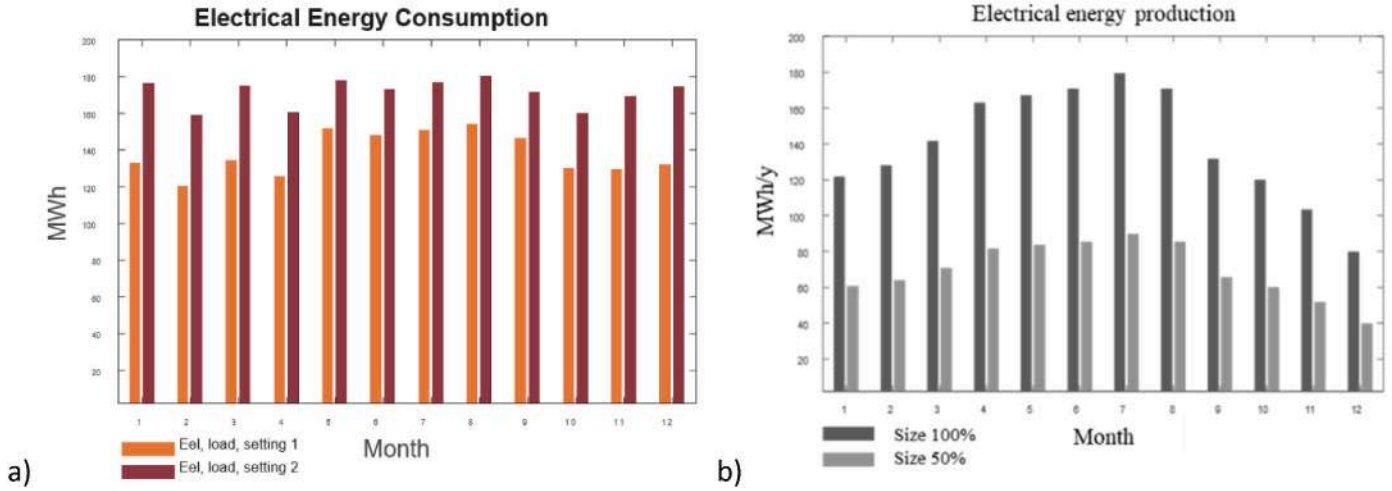

Fig. 7. a) Electrical energy consumption. b) Electrical energy production.

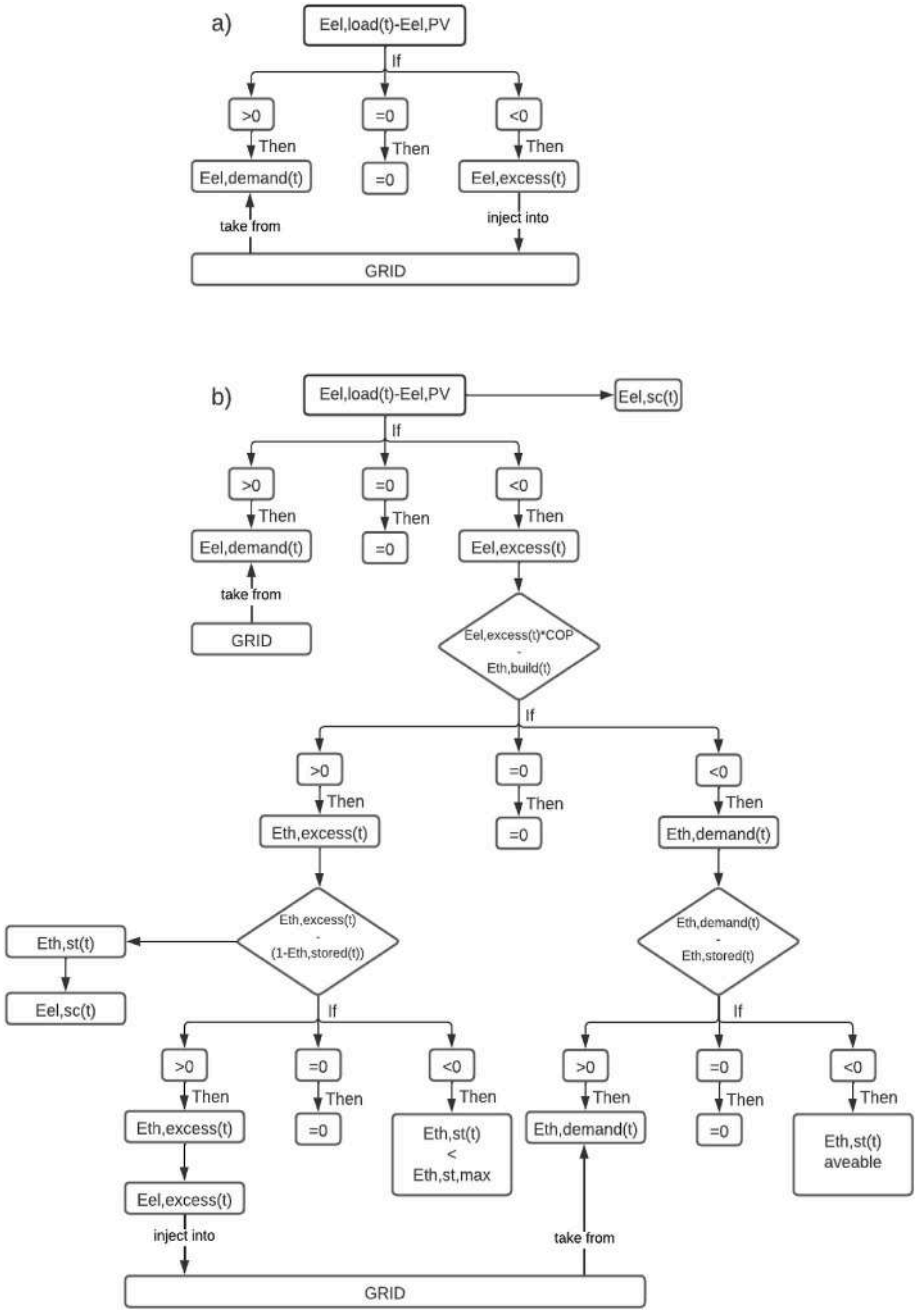

Fig. 8. Energy balance flow chart. a) scenarios without thermal energy storage. b) scenarios with thermal energy storage.

where:

$\dot{E}_{th,available\ charge,t}(t)$ is the thermal energy available to be stored in the TES, evaluated as:

$$\dot{E}_{th,available\ charge,t}(t) = \dot{E}_{th,st,max}(t) - \dot{E}_{th,st,t-1}(t) \quad (6)$$

with $\dot{E}_{th,st,t-1}(t)$ thermal energy stored in the time steps $t-1$.

If there is a thermal energy demand ($\dot{E}_{el,excess}(t) * COP - \dot{E}_{th,load}(t) < 0$), then the energy flows can be defined as follows:

$$MIN\left[\dot{E}_{th,exces}(t), \dot{E}_{th,available\ discharge,t}(t), P_{max,TES}\right] = \dot{E}_{th,discharge}(t) \quad (7)$$

where:

$$\dot{E}_{th,available\ discharge,t}(t) = \dot{E}_{th,st,t-1}(t) - \dot{E}_{th,st,min}(t)$$

If the thermal energy stored in the Thermal Energy Storage (TES) is insufficient, the system draws the necessary electricity from the grid to meet the demand.

2.4. Key performance indicators

Five Key Performance Indicators (KPIs) were assessed to compare the six REC scenarios from an energy-environment perspective.

Within the REC, the electricity produced by the photovoltaic panels will first be consumed by prosumers, then the excess will be fed into the grid to be shared with consumers for their own consumption.

Starting with the energy demand and the energy produced by the photovoltaic field, the level of energy self-consumption achieved through different configurations was considered, and a specific indicator was used for its evaluation.

The self-consumption factor (f_{SC}) was defined as the ratio of renewable energy self-consumption ($E_{el,SC}$) to the overall production

over the year ($E_{el,PVT}$).

$$f_{SC} = \frac{E_{el,SC}}{E_{el,PVT}} \quad (8)$$

In contrast to f_{SC}, the amount of energy shared with the REC as a complement to the self-consumed electrical energy was evaluated:

$$E_{el,sh,excess} = E_{el,PVT} - E_{el,SC} \quad (9)$$

It is therefore possible to define the fraction of shared energy (fsh) as the ratio between the energy shared by prosumers with the REC and actually absorbed by consumers for their own needs (E_(el,SE)) and the annual photovoltaic production ($E_{el,PVT}$).

$$f_{Sh} = \frac{E_{el,sh}}{E_{el,PVT}} \quad (10)$$

Finally, to complete the balance on the production side, it is possible to calculate the surplus of electricity produced but not absorbed by the Energy Community and injected into the grid.

$$E_{el,PV,grid} = E_{el,PVT} - E_{el,SC} - E_{el,sh} \quad (11)$$

Additionally, an indicator was defined to assess electrical self-sufficiency (f_{SS}) of the scenarios, calculated as the ratio of renewable energy self-consumption within the perimeter of the entire REC ($E_{el,SC} + E_{el,sh}$) to the overall annual electrical energy demand ($E_{el,load}$).

$$f_{SS} = \frac{E_{el,SC} + E_{el,sh}}{E_{el,load}} \quad (12)$$

To complete the energy assessment, the primary energy associated with each scenario and the corresponding Non-Renewable Primary Energy Savings (PES) were calculated by comparison with the initial state (s0), i.e., in the absence of any improvement.

$$PES = \frac{PE_{nREN,i}}{PE_{nREN,s0}} \quad (13)$$

Finally, the tons of CO_2 avoided by each scenario were assessed, taking into account the self-consumed energy from renewable sources not drawn from the national grid, and, in the case of configurations 2 and 3, the CO_2 saved through the non-combustion of fossil fuels.

3. Results

In this section, results are presented and discussed. Subsequently, in Section 3.1, model validation is conducted through a comparative analysis of electrical, DHW, and heating consumption. In section 3.2 is then reported the results of the parametric analysis in particular the section will mainly focus on the variation of the fraction of energy shared as a function of the capacity of the photovoltaic panels, the degree of electrification, the prosumer-consumer distribution and the effect of storage. Finally, in section 3.3 the results for the six specific cases described above are given. The impact of variations in production ($f_{PV} = 1$ and $f_{PV} = 0.5$) and load conditions (with and without HP) on self-consumption, self-sufficiency, and the primary energy requirement is explored. Additionally, consideration is given to how these parameters dynamically shift in cases of increased or decreased system flexibility (with or without TES). The assessment extends to the calculation of CO_2 emissions avoided for each scenario. It should be noted that economic evaluations have been devoted to a separate chapter (Section 4).

3.1. Model validation

The energy model is based on building template developed by Vallati et al. [60] that define a new paradigm of building archetype that is not only focused on the technical-architectural characteristics of the building, but is also characterised by the energy aspects. Analysing real data (e.g. usage schedule such as heating operating hours), they made it possible to represent a wide range of public residential buildings in Italy and Europe in a model building. UMI simulated all the energy loads of the examined buildings (Fig. 9).

The data export was set up to have hourly consumption for each service type (e.g. electricity, heating) for sample dwelling in respective transect and also for the entire urban area. The error in the consumption results extracted from the energy model is less than 4.7 % for each dweller for each service (Table 2), so they can be considered affordable [64].

3.2. Parametric analysis results

Variation of fraction of shared energy (fsh) in the REC as a function of installed PV power.

- Since fsh is the ratio between the energy produced and consumed within the REC itself and the total production, at the same load and as the installed power increases, the fraction of shared energy decreases to a minimum of 0.31 with a 1 MW PV system.
- The curve presents a concave downward trend with an inflection near the maximum f_{sh}. Specifically, f_{sh} is equal to 1 with an installed PV capacity of 130 kW or less (green dot Fig. 10) corresponding to 20 % of the maximum load (619 kW).

Assuming therefore the values of the fraction of shared energy (f_{sh}) shown in Fig. 10 as the base curve, we continue the analysis by looking at how the fraction of shared energy varies for different degrees of electrification and different prosumer fractions.

Fig. 11 shows the values of the fraction of shared energy (f_{sh}, top) and the fraction of self-supporting energy (f_{ss}, bottom) as the PV array capacity and the degree of electrification vary.

3.2.1. Electrification degree

Taking the basic curve in black as a reference (Fig. 11) with PVcapacity from 1 to 1000 kW, $E_{dg} = 0$ and $Pdg = 0$ and analysing the variation of the fraction of shared energy f_{sh}, it can be seen that as the degree of electrification increases, f_{sh} increases with the same photovoltaic production, reaching a minimum value of 0.42 with $PV_{capacity} = 1$ MW and raising the maximum threshold with $f_{sh} = 1$ from 150 kW to 250 kW, rising from 24 % of maximum load to 40 %.

Relating consumption from solar sources no longer to production, but to electricity demand, one finds an inverse f_{ss} trend, as production increases, the fraction of load coverage from solar sources increases to a maximum of 35 %.

Analysing the course of the curves, it can be seen that the self-support (f_{ss}), grows differently, and therefore with different slopes, depending on the degree of electrification, arriving at an intersection in the curves around 750 kW of installed photovoltaic power, leading the curve with $E_{dg} = 1$ corresponding to a maximum f_{ss} with less photovoltaic capacity to become the case with less f_{ss} with maximum installed capacity.

Overall, the increase in installed capacity is true that it leads to an increase in self-supply, but at the same time it leads to a higher fraction of energy fed into the grid ($f_{sg} = 1$-fsh), In the borderline case of 1 MWh, there is a minimum of 55 % to a maximum of 70 % of energy produced and fed into the grid, thus undermining the very concept of the REC, whose objective is, on the one hand, to produce satisfying electrical loads by means of renewable resources, but also to manage these resources rationally, rewarding consumption within the REC itself without overloading the grid.

Setting the limit of $f_{sh} = 1$, the maximum photovoltaic capacity that can be installed is 150 kW (dot black vertical line Fig. 11), as shown above, to which corresponds an f_{ss} that varies from 0.13 to 0.17 depending on the degree of electrification. With reference to the load profile of the residential archetype illustrated above, setting an f_{sh} equal to 1, therefore with no surplus to the grid, the maximum coverage from renewables obtainable through the installation of photovoltaic panels

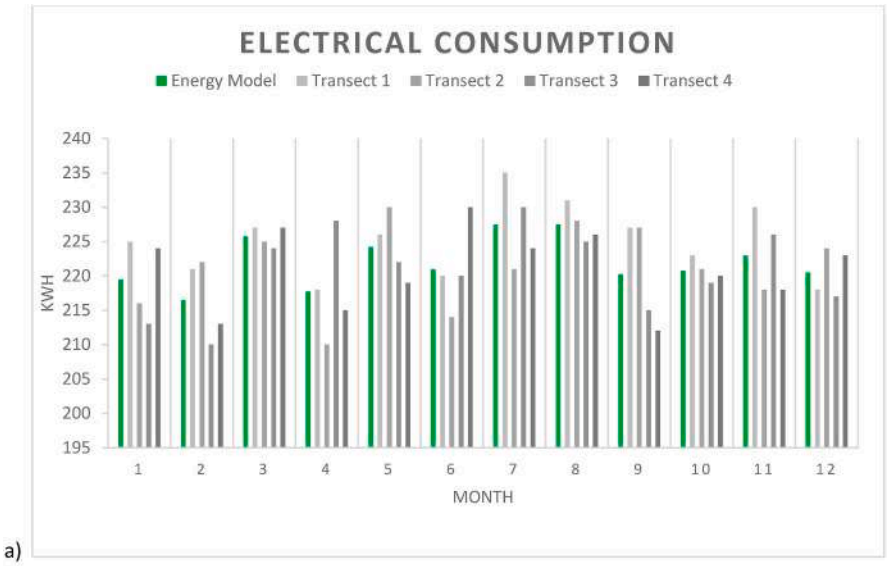

a)

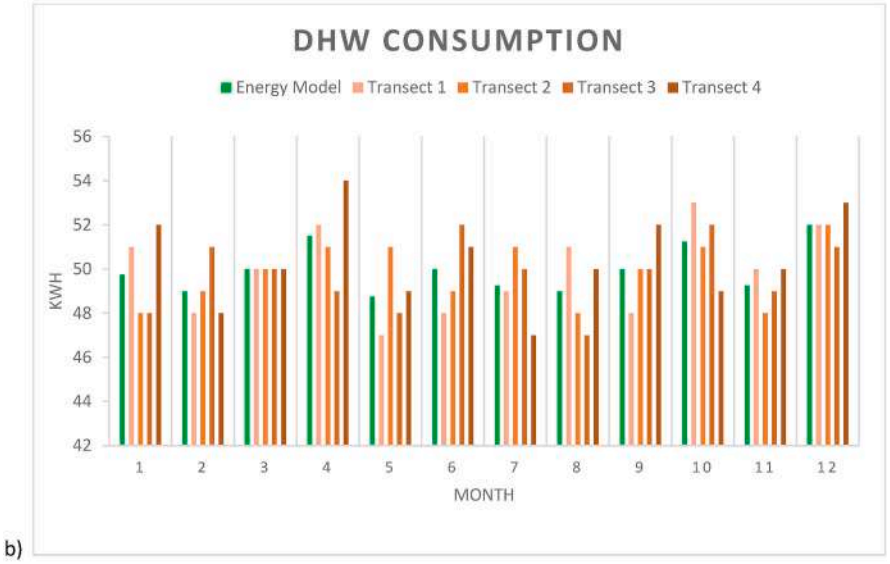

b)

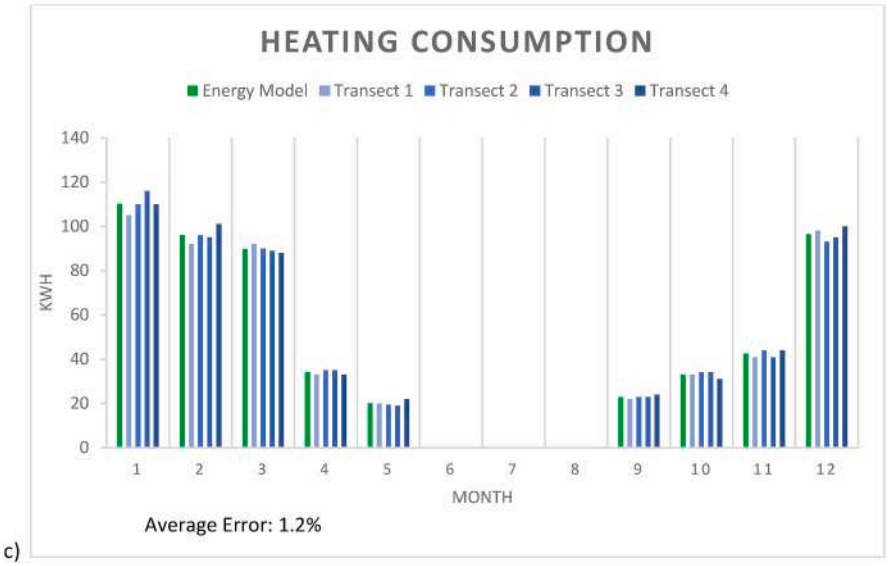

c)

Fig. 9. Model validation a) Electrical consumption, b) DHW consumption, c) heating consumption.

Table 2
Comparison between digital model and real data for each service.

Month	Electrical consumption error [%]				DHW consumption error [%]				Heating consumption error [%]			
	B1	B2	B3	B4	B1	B2	B3	B4	B1	B2	B3	B4
1	2.5 %	−1.6 %	−3.0 %	2.1 %	2.5 %	−3.5 %	−3.5 %	4.5 %	−4.8 %	−0.2 %	4.8 %	−0.2 %
2	2.1 %	2.5 %	−3.0 %	−1.6 %	−2.0 %	0.0 %	4.1 %	−2.0 %	−4.2 %	0.0 %	−1.0 %	4.2 %
3	0.6 %	−0.3 %	−0.8 %	0.6 %	0.0 %	0.0 %	0.0 %	0.0 %	2.5 %	0.3 %	−0.8 %	−1.9 %
4	0.1 %	−3.6 %	4.7 %	−1.3 %	1.0 %	−1.0 %	−4.9 %	4.9 %	−2.9 %	2.9 %	2.9 %	−2.9 %
5	0.8 %	2.6 %	−1.0 %	−2.3 %	−3.6 %	4.6 %	−1.5 %	0.5 %	−0.6 %	−3.1 %	−4.6 %	9.3 %
6	−0.5 %	−3.2 %	−0.5 %	4.1 %	−4.0 %	−2.0 %	4.0 %	2.0 %	0.0 %	0.0 %	0.0 %	0.0 %
7	3.3 %	−2.9 %	1.1 %	−1.5 %	−0.5 %	3.6 %	1.5 %	−4.6 %	0.0 %	0.0 %	0.0 %	0.0 %
8	1.5 %	0.2 %	−1.1 %	−0.7 %	4.1 %	−2.0 %	−4.1 %	2.0 %	0.0 %	0.0 %	0.0 %	0.0 %
9	3.1 %	3.1 %	−2.4 %	−3.7 %	−4.0 %	0.0 %	0.0 %	4.0 %	−4.3 %	0.0 %	0.0 %	4.3 %
10	1.0 %	0.1 %	−0.8 %	−0.3 %	3.4 %	−0.5 %	1.5 %	−4.4 %	0.0 %	3.0 %	3.0 %	−4.1 %
11	3.1 %	−2.2 %	1.3 %	−2.2 %	1.5 %	−2.5 %	−0.5 %	1.5 %	−3.5 %	3.5 %	−3.5 %	3.5 %
12	−1.1 %	1.6 %	−1.6 %	1.1 %	0.0 %	0.0 %	−1.9 %	1.9 %	1.6 %	−3.6 %	−1.6 %	3.6 %

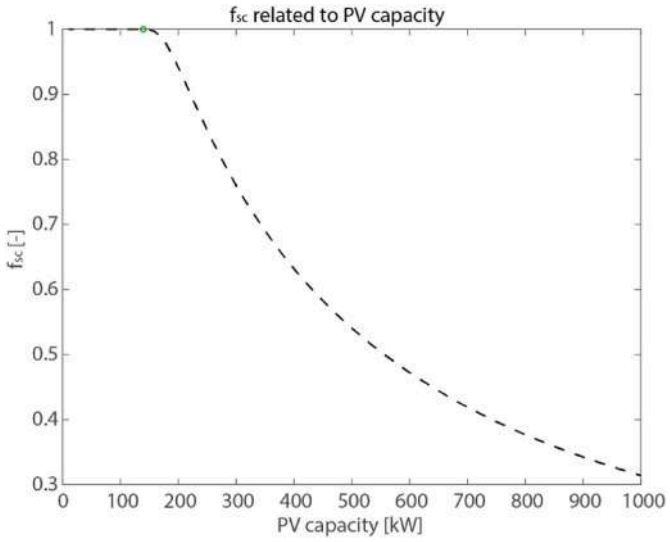

Fig. 10. Variation of f_{sh} related to the installed photovoltaic capacity.

and electrification of electricity consumption is 17 %.

3.2.2. Prosumer-consumer distribution

Starting from the base case and instead varying the percentage of prosumers and consumers within the REC, it is possible to analyze the respective variations in terms of energy shared and energy self-consumed by prosumers (Fig. 12).

Compared to the base case (black curve in Fig. 12) where all users are considered consumers, as the percentage of prosumers within the energy community increases, the energy produced and consumed within the perimeter shifts from being shared energy used by consumers to self-consumed energy consumed by prosumers. Looking at the two graphs in Fig. 12 and the values of f_{sh} and f_{ss} we see that the sum of the two fractions for each combination of PV capacity and prosumer is equal to the value, at the same points, of the base case. All the way to the limit case where the f_{sc} curve with prosumer equal to the entire user coincides with the f_{sh} curve of the base case itself (prosumer = 0).

Starting from the base case up to 150 kW PV capacity the energy produced is entirely absorbed by the REC, depending on where one stands if on the limit case prosumer = 0 one will have $f_{sh} = 1$ or in the limit case prosumer = 1 one will have $f_{sc} = 1$. In all other cases where the energy community has a different mix between consumer and prosumer, a peak in the f_{sh} profile between 150 and 230 kW is identifiable, as can be seen in more detail in Fig. 12. As the proportion of consumers considered as prosumers increases, the peak drops and shifts to the right.

Since there is no excess energy to the outside of the ERC up to this limit value, all the energy produced is consumed first by prosumers and then by consumers; therefore, as the capacity of the panels increases up to the peak value, there is an upward trend in shared energy. Beyond the peak, the energy produced is such that there begins to be a surplus, and the trend in the fraction of energy shared becomes decreasing, as does the fraction of energy self-consumed. If the energy fed into the grid is taken into account, it will be zero until the peak is reached for each different prosumer-consumer distribution within the REC, and then continues on an upward trend.

Regardless of the composition of the REC, in terms of prosumer and consumer, given the load profile, it is possible to identify a maximum photovoltaic capacity such that the maximum fractions of shared and self-consumed energy, as well as the minimum with respect to release to the grid, are obtained. In the case under consideration, given the productivity of the panels, the horizontal radiation of 1924.32 kWh/m2 and the load profile of the residential archetype described above, these optimum values lie at approximately 1/4 of the maximum load.

3.2.3. Thermal storage

As described above, the fractions of shared and self-sustaining energy were then evaluated considering the introduction of thermal storage.

The two approaches note the desired level of electrification and PV capacity by sizing heat pumps and thermal storage differently. In particular, the first approach (A1) focuses on electrical production from renewables and on maximizing self-consumption, while the second (A2) focuses on the thermal load and the down size of the HP, leaving the thermal storage to manage the building's load dynamics. In fact, as a result of the two sizing approaches, with the same degree of electrification and photovoltaic capacity, the first approach (A1) results in a greater maximum capacity to be met with HPs than the second approach (A2) and smaller volumes for thermal storage (Fig. 13). Furthermore, while with the first approach HPs and TESs vary as the photovoltaic panels and the degree of electrification change, with the second approach they are independent of the size of the solar field.

Once the total capacity of the HPs and TESs for both approaches had been identified, it was possible to evaluate the fraction of shared energy (f_{sh}) and self-sustaining energy (f_{ss}) achieved through the inclusion of the thermal reservoirs so as to compare the results previously obtained in the absence of the TESs, as well as the two approaches with each other. It should be noted that, for computational reasons, the scenarios with the presence of the thermal reservoirs were always evaluated at varying photovoltaic capacity, but for only one degree of electrification with E_{dg} equal to 1.

Fig. 14 shows the transformations of the reference curve (black dot line, base case, with $E_{dg} = 0$ and $V_{TES} = 0$) first following electrification alone (orange dot line, with $E_{dg} = 1$ and $V_{TES} = 0$) and then following the inclusion of thermal storage through the two different approaches.

The first approach (A1, light green line) sees a general increase in the fraction of energy shared and a linearisation of the curve as the PV capacity changes. This leads to a shift of the maximum ($f_{sh} = 1$) at a total installed PV capacity of 600 kW, and an increase of the minimum value

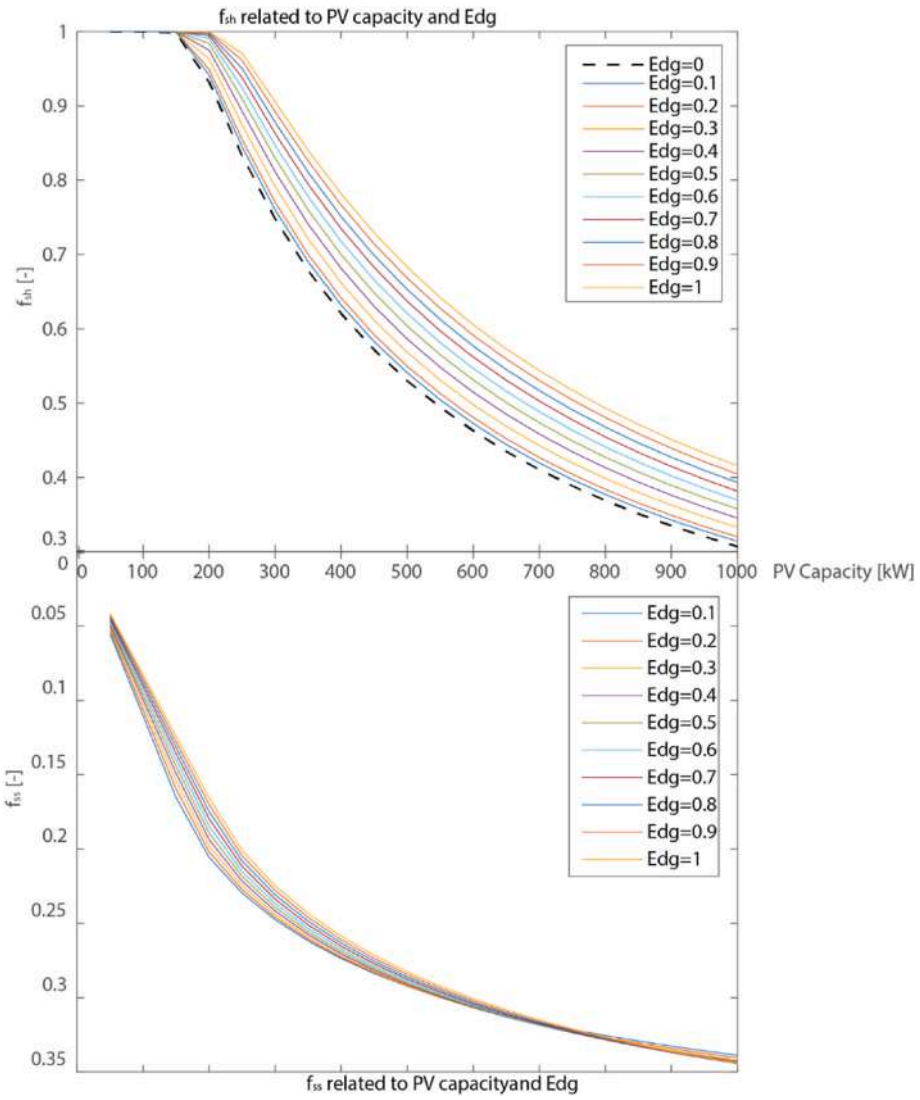

Fig. 11. Shared energy fraction and self-sufficiency fraction related to PV capacity and electrification degree (E_{dg}).

to $f_{sh} = 0.5$ (PV capacity = 1000 kW (maximum)). While the maximum increase in the fraction of shared energy is at 600 kW and is +0.33 compared to the base case and +0.18 compared to the same electrification share but without TES.

The second approach (A2, dark green line) from the point of view of shared energy is such that it does not bring a significant improvement over electrification alone. This is because both the operating logic and the sizing of the HP and TES are not designed to optimize the energy shared and consumed within the REC itself.

With the same degree of electrification and therefore load ($E_{dg} = 1$ and A1), the two curves (dot orange and light green) relating to the fraction of self-sufficiency (f_{sh}) are coincident until f_{sh} is equal to 1, after which a clear gap is seen between the first curve (without storage) and the second where the presence of storage allows for further significant growth up to 450 kW. Using the A2 approach, having a down-size of HP, despite the same degree of electrification as in the two previous scenarios ($E_{dg} = 1$) results in a lower total annual consumption, moving closer to the base case.

The inclusion of thermal energy storage (power-to-heat) leads to an increase in the energy shared and consumed within the REC itself. A comparison of the two approaches (A1 and A2) of sizing storage capacity and HP from an energy perspective shows a strong positive bias towards the former. In a full comparison, the ease of implementation of the two different approaches should also be taken into account, as each of them brings with it different control logics and plant configurations.

3.3. Specific case study

As previously mentioned different heat pump capacities, PV and TES, lead to a variation of the results. In this section it was decided to consider two different values for PV, to maintain the fixed thermal capacity of HP equal to the maximum load required by the building, as well as to maintain a fixed value for TES, selected based on the following parametric analysis.

The volume of the TES has been made to vary from a range ranging from 10 to 1000 m^3 for both configurations of PVT ($f_{PV} = 100$ e $f_{PV} = 50$) evaluating the variation of self-consumption, self-support, as well as the change in the cost of the TES itself.

It is necessary to emphasized that in this phase of the analysis is considered a dedicated pod for electricity production, therefore, being the load of the prosumer close to zero, the energy produced becomes all shared energy. The focus will be on exchanges between REC and network, not on internal energy exchanges within the REC (as previously), but on exchanges between RECs and networks, so that the term self-consumption (SC) will be used as a synonym for shared energy, while with "energy fed into the grid" or "shared with grid" it refers to the

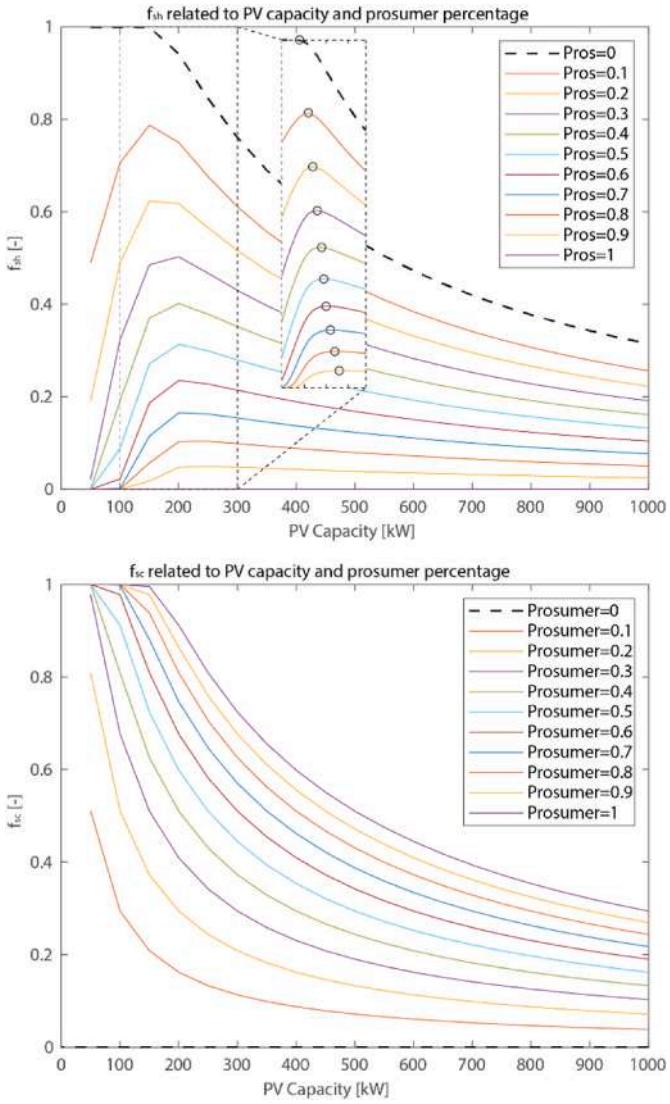

Fig. 12. variation of shared energy fraction (f_{sh}, figure a) and self-consumption fraction (f_{sc}, figure b) related to variation of PV capacity and prosumer percentage.

energy exchanged from the REC to the network and not to the shared energy (Shared-energy) between prosumer and consumer at the internodal of the REC itself.

Fig. 15 shows changes in SC (a), SS (b), PES (c) and tCO_2 avoided equivalents (d) as the volume of TES varies for both PV sizes. All curves have an almost linear section in which as the volume of storage increases the investigated parameter, a connecting part where there is a variation of the slope of the curve, that is, the increase of the KPI as the volume increases and in the end the curve tends to become asymptotic to the maximum value reached with the specific configuration. In this case, high performance increases occur with values below 200 m^3. Between 200 and 300 m^3 the increase decreases to reach a delta close to 0 over 300 m^3.

Considering the cost of the panels as the volume varies according to equation (12) [26,65] and comparing it with the above KPI values (Fig. 16) above 200 m^3 the curve changes concavity and the price increase, linked to the volume increase, does not correspond to a significant increase in performance. A volume for s3 and s4 scenarios of 200 m^3 was then selected.

$$COST_{TES=}4042\ V_{TES}^{0.506} \tag{12}$$

3.3.1. Effects on self-consumption

Before analysing the results, it should be specified that in this case self-consumption refers to all the energy self-consumed within the REC, i.e. the energy self-consumed by prosumers plus the energy shared and absorbed by consumers. because at this stage of the analysis we are not going to characterize the prosumer-consumer distribution within the REC itself.

Interpolating production and hourly consumption data over the year, for the six scenarios the share of self-consumed electricity was determined: 34 %, 42 %, 58 %, 57 %, 68 % and 96 % respectively (Fig. 17). The variation of self-consumption share is influenced by changes in energy demand and by the size of the photovoltaic system (PV), to which reference can be made in terms of photovoltaic fraction (Eq. (13))

$$f_{PV=}\frac{\mathrm{Eel,PVT}}{\mathrm{Eel,load}} \tag{13}$$

Where Eel, PVT is the annual energy production from PV and Eel, load the annual REC's electricity need.

The increase in electrical load (Fig. 18), which due the introduction of HP passes from 1.7 GWh (s1 and s4) per year to 2.1 GWh (s2 and s5) per year (+19.4 %), results in a directly proportional increase in energy self-consumption (SC). In fact, between s1 and s2 there is a positive SC change of 9 %, similarly between s2, s5 counting 11 % (Fig. 17).

On the other hand, PV system size affects (Fig. 17) 24 % in the s1/s4 comparison and 26 % in the s2/s5 comparison: the increase of self-consumption with the reduction of the PV size is more evident in systems where the production of electricity from PV is more distant from satisfying the electrical load, namely has lower photovoltaic fraction (f_{PV}).

This gives an indication of how the right sizing of the solar field has its importance, pointing out that an oversizing is not in favor of achieving efficiency goals.

Indeed, increasing electricity production, does not automatically lead to a significant rise in the self-consumed energy; essentially the curve has a horizontal asymptote.

In s5, although the electric production is halved, the self-consumed electric energy is 4 % higher than the self-consumption in s1.

The use of thermal storage enables the PV system to store the excess electrical energy generated beyond the instantaneous electrical load. The stored energy can then be used during times when the PV production is insufficient to meet the load. This practice significantly enhances self-consumption as it enables using self-generated energy during times when grid dependency is prevalent.

The use of thermal storage enables the PV system to store the excess electrical energy generated beyond the instantaneous electrical load. The stored energy can then be used during times when the PV production is insufficient to meet the load. This practice significantly enhances self-consumption as it enables using self-generated energy during times when grid dependency is prevalent. Such a result is consistent with the existing literature, which shows that heat pumps combined with thermal energy storage can increase system flexibility [66]. Furthermore, the potential for RES integration is consistent with what has been analyzed in previous work by some of the authors of this article [26].

Analyzing the third setting for the implementation of thermal storage, the self-consumption increases by 6 % when comparing s2-s3 (100 % energy need) and s5-s6 (50 % energy need). This results in an electrical self-consumption of 41 % for s3 and 34 % for s6 (Fig. 17).

3.3.2. Effects on shared-energy from REC to grid

As specified in the previous section, in this analysis the entire perimeter of the REC is taken into account without going on to define internal flows, thus distinguishing between self-consumed and shared energy between prosumers and consumers. Therefore, it is specified that the term "shared-energy" is referring to the electricity fed into the grid by the community.

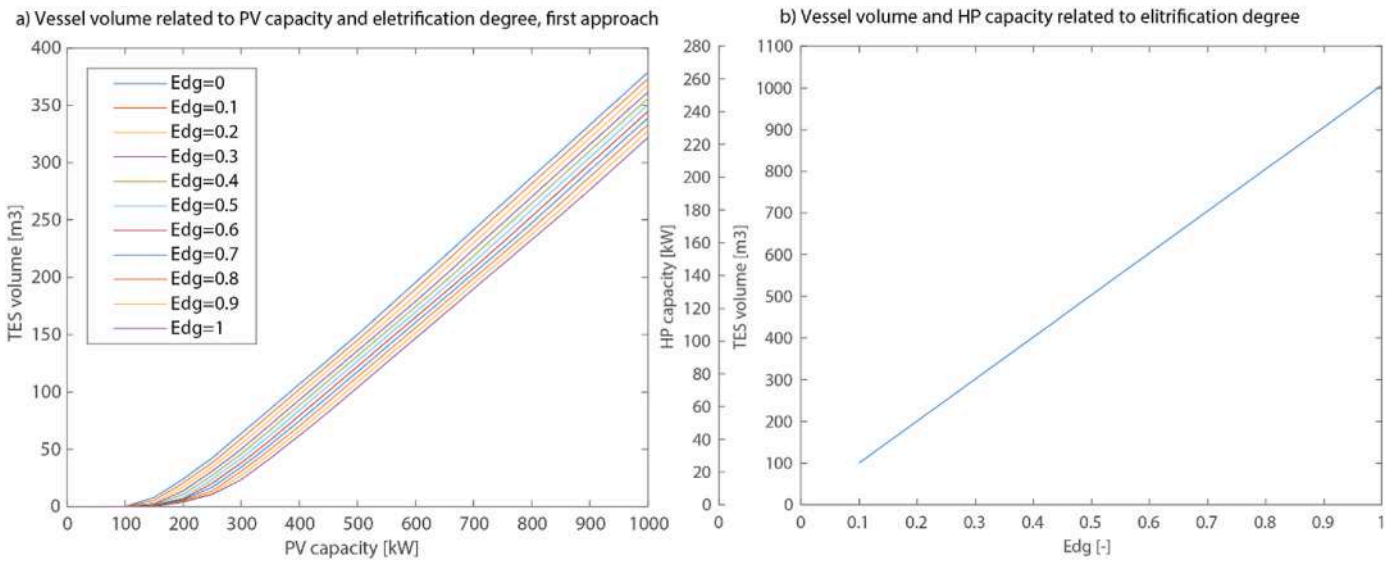

Fig. 13. Vessel volume and HPs capacity request by first (a) and second (b) approach.

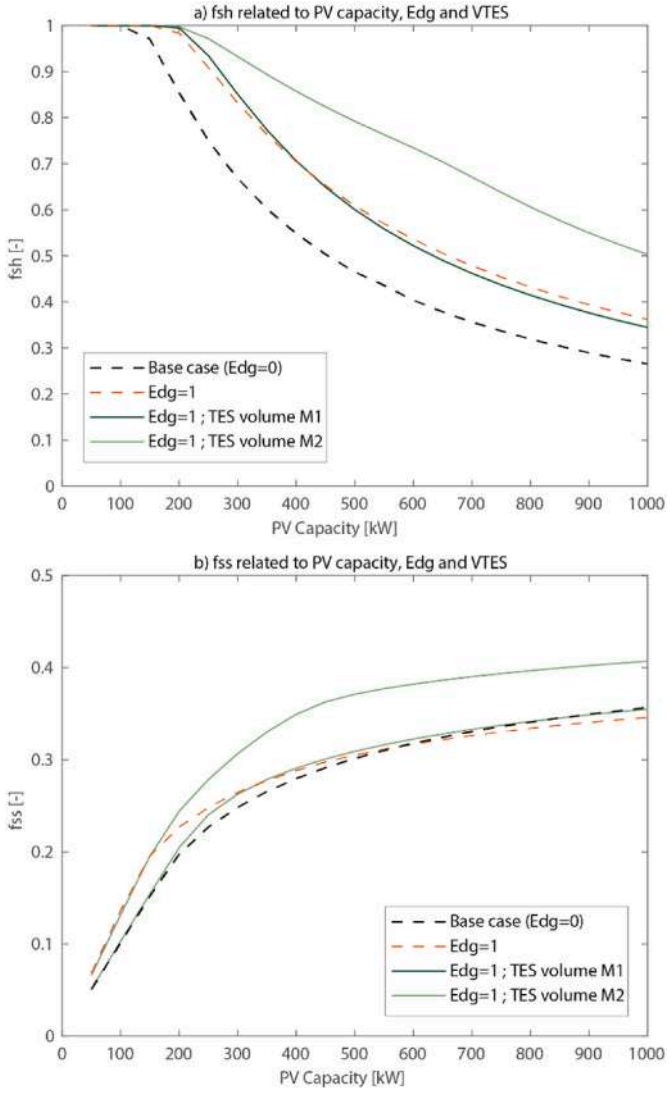

Fig. 14. Shared energy fraction (f_{sh}) related to PV capacity in four different configurations.

Simulating a photovoltaic system sized to cover 50 % of the total energy demand (s4 and s5) clearly results in high values of self-consumed (SC) energy, in terms of self-consumption fraction, but also in a decrease in energy fed into the grid (Fig. 17).

In detail, the difference between the scenarios s1 and s4 is a slightly lower amount of MWh self-consumed, decreasing by 14 %, against a decrease in MWh of shared energy (SE) by 67 %.

Similarly comparing the s2 scenario and the s5 scenario, MWh of self-consumed energy decrease by 17 % with a collapse of MWh of energy shared in the grid by 72 %.

It is evident that electrification of consumptions results, within an energy community setting, in increased self-consumption and lower network disturbance, as opposed to the installation of higher electrical power capacity.

Examining the effects of electrical load and PV size, focusing on non-renewable primary energy, the change in energy behavior due to the inclusion of thermal storage is remarkable. This results in a notable increase in energy utilization, with self-consumption rates reaching 58 % and 96 % for s3 and s6, respectively. Comparison between s2 and s3 shows a 16 % increase, while comparing s5 and s6 reveals a 28 % increase, both of which were recorded in the third setting (Fig. 17).

The results show that high levels of self-sufficiency in a residential energy system are difficult to achieve even with high renewable generation. As demonstrated in Ref. [67], several generation and storage energy systems need to be interconnected in order to have a substantial increase in system self-sufficiency.

3.3.3. *Effects on self-sufficiency*

In Fig. 18, the electrical energy consumption is depicted, divided into self-consumption ($E_{el,SC}$ MWh/y) and the energy request to the grid ($E_{el,DG}$ MWh/y) to satisfy the electrical demand. The self-sufficiency fraction (f_{SS}), determined by the ratio between self-consumption and total electrical consumption, signifies the system's capability to meet the electrical demand through renewable electricity generated by the PV system. The self-sufficiency factors for the six scenarios were determined as follows: 0.34 (s1), 0.34 (s2), 0.47 (s3), 0.29 (s4), 0.28 (s5), and 0.39 (s6) respectively (Fig. 18). The subsequent analysis explores how f_{SS} is influenced by variations in load, production, and the matching between production and load.

With constant production, transitioning from scenarios with setting 1 (s1 and s4) to scenarios with setting 2 (s2 and s5) results in a simultaneous increase in the building's load and self-consumption (Fig. 18), both values being 19 %. This leads to a negligible change in f_{SS}.

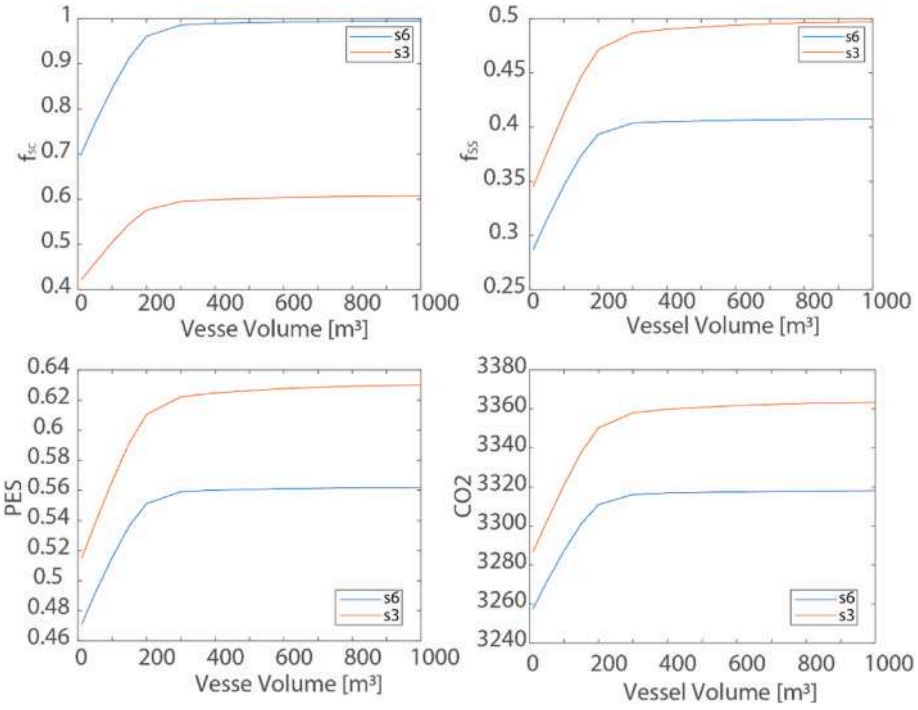

Fig. 15. Variation of different KPI related to the vessel volume (TES Volume). a) Self consumption fraction (f_{SC}), b) self-sufficiency fraction (f_{ss}), c) Primary Energy Saving (PES); d) equivalent CO_2 ton avoided (tCO_2 avoided).

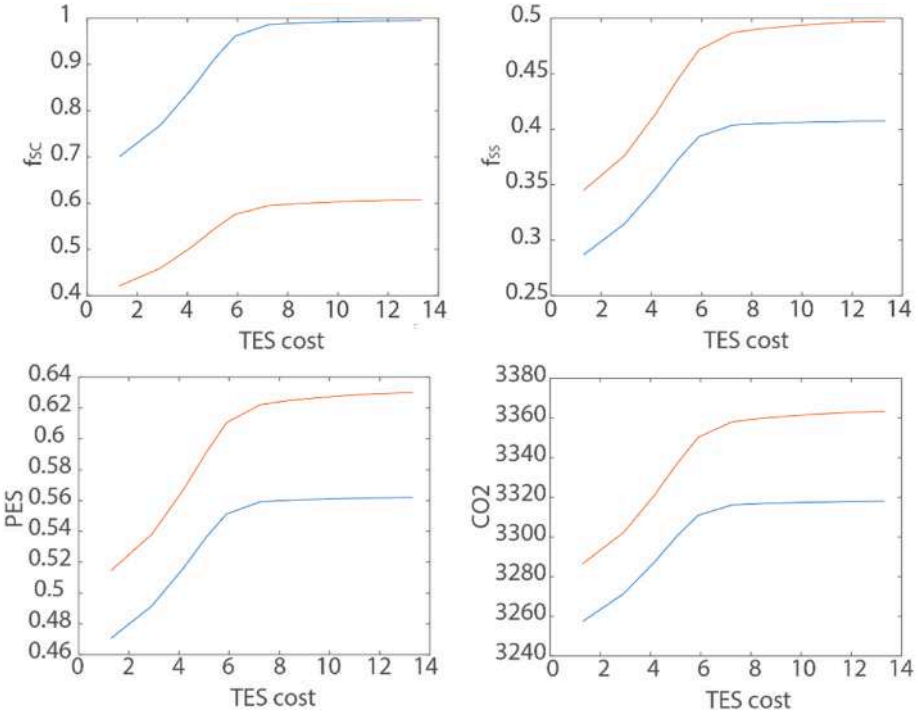

Fig. 16. Variation of different KPI related to the vessel cost a) Self consumption fraction (f_{SC}), b) self-sufficiency fraction (f_{ss}), c) Primary Energy Saving (PES); d) equivalent CO_2 ton avoided (tCO_2 avoided).

Conversely, introducing Thermal Energy Storage (TES) (s3 and s6), while maintaining the same energy demand, leads to an increase in self-consumption and, consequently, self-sufficiency. There is an 42 % increase from s1 to s3 and 41 % increase from s4 to s6.

3.3.4. *Effects on PE,nren*

In addition, the Primary Energy demand and the impact of non-renewable primary energy of the six scenarios was evaluated compared to the ante-operam (Fig. 19). The comparison with the ante-operam (s0) shows a decrease in non-renewable primary energy of 17%–20 % for s4 and s1; to 45%–50 % in case of electrification proposed by s5 and s2 respectively; to 60%–54 % achieved with the implementation of a storage in s3 and s6. The difference between s1 and s4, shows that when used nonrenewable sources for heating and domestic

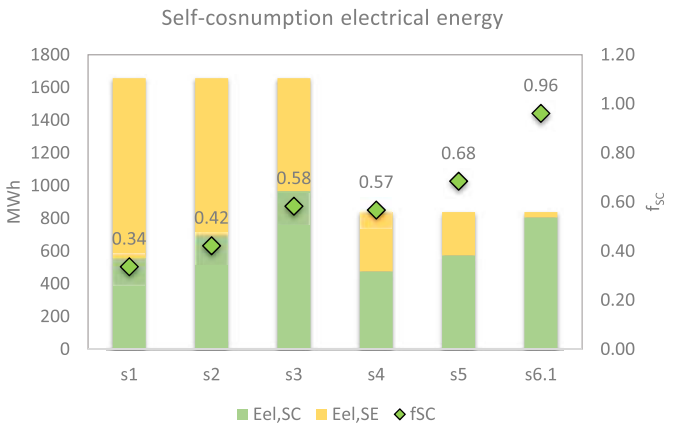

Fig. 17. In the left axis the self-consumption energy (green bar, $E_{el,SC}$) and the electrical energy shared to the grid (yellow bar, $E_{el,SE}$), are reported in MWh; the sum of the two energy contributions is the total energy production by the PV plants. In the right axis the self-consumption factor (f_{sc}) is shown.

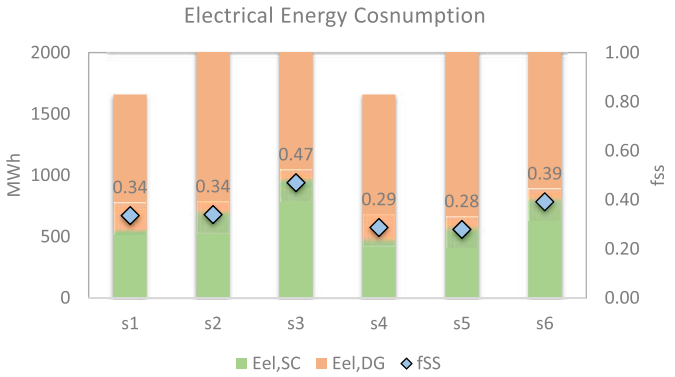

Fig. 18. In the left axe are, in MWh, the self-consumption energy (the green bar, $E_{el,SC}$) and the electrical energy request to the grid (orange bar, $E_{el,DG}$), the sum of the two Energy is the total energy consumption by the building. In the right axe is shown the self-sufficiency factor (f_{ss}).

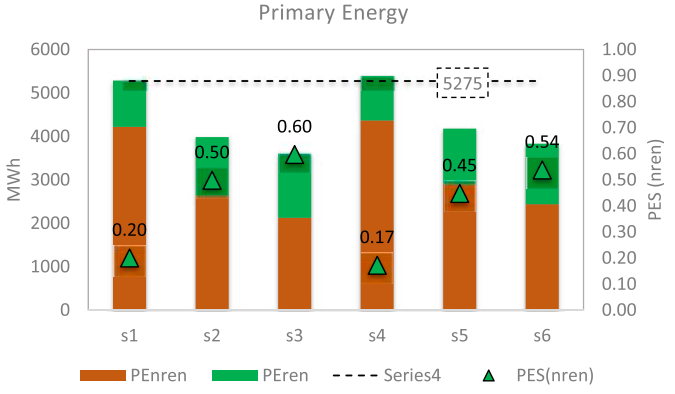

Fig. 19. Primary energy demand. Left axis, in MWh: No renewable primary energy (dark orange bar, PE_{nREN}) and renewable primary energy (dark green bar, PE_{REN}), the sum of the two energy is the total Primary Energy consumption (PE) by the building. In the right axis the primary energy saving (PES) is shown.

hot water, doubling the size of the photovoltaic system leads to a decrease in nonrenewable primary energy of only 3 % (s1/s4).

Conversely, when taking advantage of different technologies, electrifying the heating and hot water loads (s2 and s5), to install a double photovoltaic power means a reduction of nREN primary energy

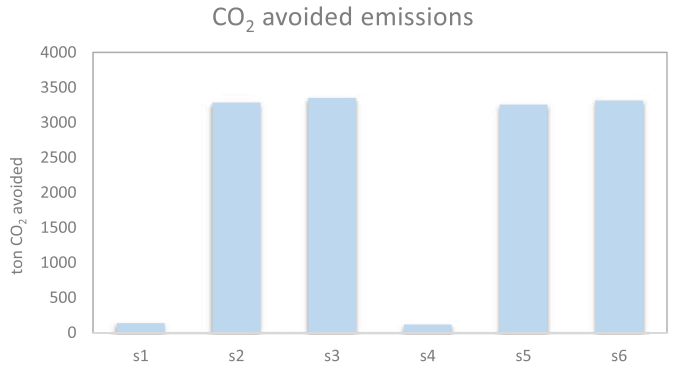

Fig. 20. CO_2 avoided emissions.

consumption by 25 %. This penalization in terms of $PE_{,nREN}$ which occurs reducing PV plant size (s5), however must be considered in relation to the simultaneous increase that is obtained in self-consumption (from 0.42 of s2 to 0.68 of s5), therefore to the least stress to which the network is subjected.

In any case, the inclusion of thermal storage increases performance by 10 % and 9 % respectively over the previous setting for both 100 % and 50 % PV sizes.

In s1 and s4, the reduction in non-renewable primary energy is solely attributed to the impact of self-consumed energy, as heat production for domestic hot water and space heating remains tied to the combustion of fossil fuels. With the replacement of boilers with heat pumps (HP), there is a minimal increase of 28 % (from s4 to s5) in non-renewable primary energy consumption, primarily due to the electrification of consumption. In fact, the transition from s1 to s2 and from s4 to s5 is four to six times greater than the transition from s2 to s3 and s5 to s6. Numerically, this translates from a non-renewable primary energy consumption of 39 % (from s1 to s2) and 28 % (from s4 to s5) to values of 10 % and 9 %, respectively, when transitioning from s2 to s3 and s5 to s6.

Finally, tons of CO_2 non-emitted were computed by considering the energy used from on-site production by PV (Fig. 20), which corresponds to the same amount of energy not harvested from the grid. By implementing the system with the heat pump, there is an increase in non-emitted CO_2. In particular, it is interesting to point out that with a 50 percent PV size feeding the heat pump, there is a reduction in GHG emissions comparable to s3.

4. Economic assessment

In support of energy and environmental analyses, the six scenarios were compared from an economic point of view. The settings can be categorized into two groups, characterized by different PV factors, $f_{pv} = 1$ and $f_{pv} = 0.5$ respectively; within each group, the variable considered is the increasing amount of technological integration interventions.

The investments effectiveness was evaluated in terms of annual costs (ACs), calculated following Equation (13) and expressed in €/yr:

$$AC = CAPEX \bullet crf + C_{O\&M} + C_{EP} \quad (14)$$

Here, CAPEX is the Initial Capital Expenditure (€), $C_{O\&M}$ refers to operation and maintenance costs (€/yr) and C_{EP} refers to energy vectors

Table 3
Economic assumptions.

	Reference amount	CAPEX	O&M cost/CAPEX
PV 100	393 kWp	357630	1.58 %
PV 50	197 kWp	156158	1.58 %
AWHP	804 kW	570840	5.84 %
FC	12 circuit, 3600 FC	185216	0.70 %
TES	200 m^3	59009	0.70 %

purchase (€/yr); crf is the capital recovery factor, defined from the interest rate of investments, i (%), and the lifetime, τ (yr):

$$crf = \frac{i \bullet (i+1)^{\tau}}{(i+1)^{\tau} - 1} \tag{15}$$

In Table 3 the detail of the parameters considered for the selected scenarios is depicted, in accordance with the assumptions outlined in Table 1.

The CAPEX was assessed in different ways for the main technologies involved in the study. The Initial Capital Expenditure related to PV was deduced from the correlation developed in Ref. [26], defining the unit investment cost versus the plant size expressed in kWp; similarly for AWHP the cost curves CAPEX/kWth in Ref. [26] were used. The value in Table 3 refers to 12 AWHP installed in the building complex. In order to assess the CAPEX of TES system, a cost function depending on the storage volume can be applied [26]. Concerning the initial expenditure for the distribution system, a fixed amount for each circuit equal to 3467.66 € was considered, to which 39.87€ were added for each terminal, in accordance with the tariff of prices of the Lazio region [68].

The considered circuits are one for ASHP and each apartment was assumed equipped with 3 terminals, resulting in total of 3600 fan-coils. To the investment cost, energy vectors purchase (CEP) and operation and maintenance costs (CO&M) were added in Equation (1). CEP of 2023 was deducted for electric energy from Ref. [69] and equal to 28.29 c€/kWh/y, whilst for operation and maintenance cost reference was made to the CAPEX percentages in Ref. [26].

To determine the AC for the various REC set ups, the investments were calculated over a time frame of 25 years, corresponding to the estimated systems' service life.

Ultimately for s1, s2 and s3 scenarios the overall CAPEX is equal to 357′630 €, 1′113′686 € and 1′155′238 € respectively; the remaining scenarios vary for the different amount of PV, with a reduced power to 197 kWp, producing electricity equal to half of the REC's annual demand.

Fig. 21 relates the annual cost to key performance indicators assumed in Section 2.3 as well as to avoided CO_2 emissions.

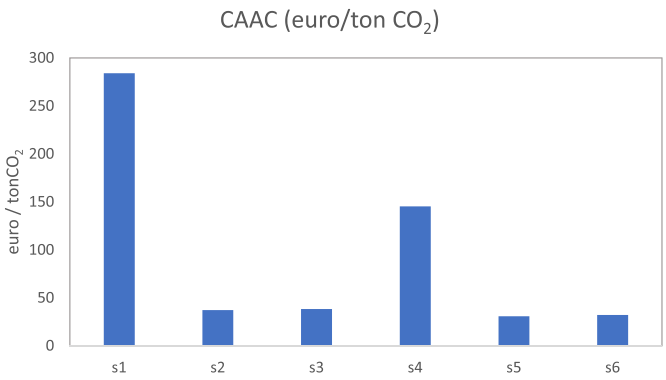

Fig. 22. Carbon avoidance annual cost (CAAC).

Limiting the investment only to the integration of RES via PV plant (s1, s4) appear the most convenient solution looking at the f_{ss}: in fact, electrifying the consumptions (s2, 24), against significant differences in the AC, f_{ss} remains nearly unchanges. This is because, as seen in Section 3.4, the increase in SC allowed by HPs and the increase in electrical load due to their introduction have the same order of magnitude. Opting for this solution requires TES to increase f_{ss} (Fig. 21 b).

The benefits of HP integration can instead be seen in terms of f_{SC}, for the same Eel, PV production, as highlighted in Fig. 21 a. Under this aspect, the photovoltaic size equal to 50 % of the base load allows to have in s6 the best self consumption factor with a sustainable investment.

As expected, the best ACs-PES results were obtained, in the case of the power plant at maximum power, for the s2 and s3 scenarios; the halved PV plant allows reduced PES, which can be balanced only by a low annual cost (s4) (Fig. 21 c).

To figure out the CO_2 emissions avoidance cost over a year related to the different configurations, Carbon Avoidance Annual Cost (CAAC)

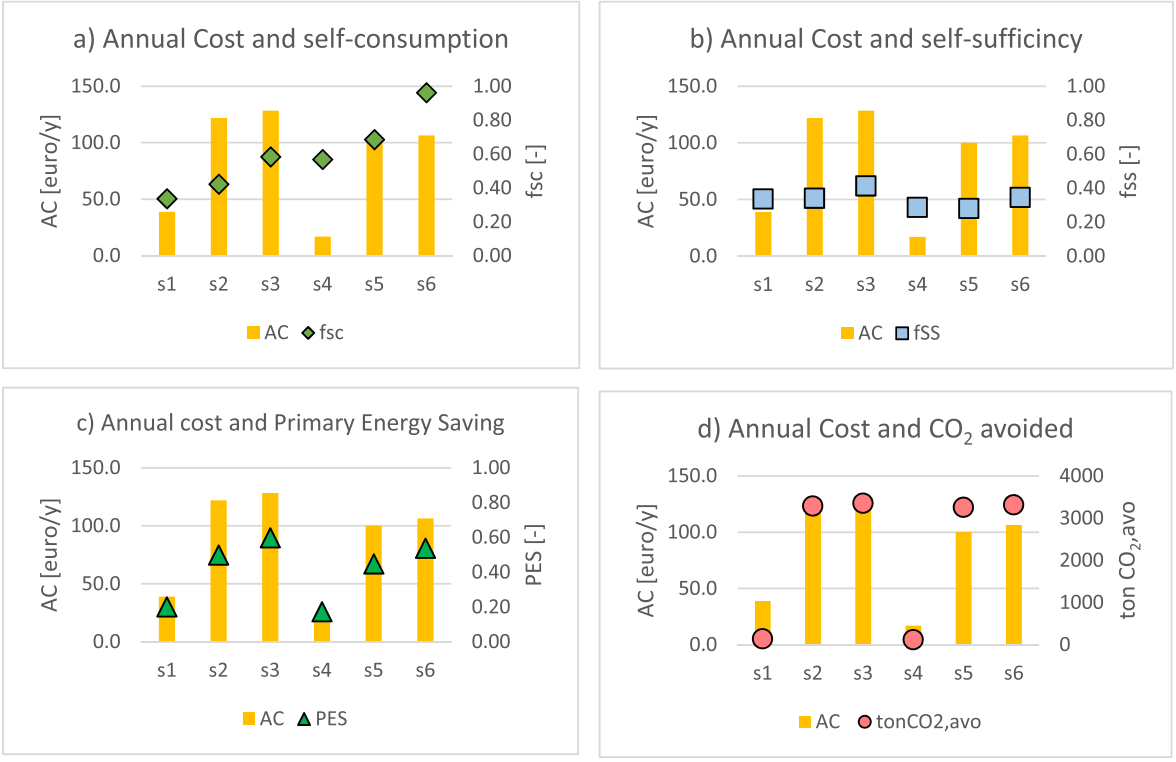

Fig. 21. Annual cost related to self-consumption fraction (a), self-sufficiency fraction(b) primary energy saving (c) and CO_2 avoided (d).

indicator was proposed. It represents the annual cost to be invested for avoiding a ton of CO_2 (€/tonCO2), and is determined as follows:

$$CAAC = \frac{AC}{AnnualCO_{2,Avd}} \tag{16}$$

As can be seen in Fig. 22, s1-s4 are the less favorable scenarios; in fact, although they require a very low initial investment, which results in an equally modest annual cost, at the same time they are those that guarantee less CO_2 savings (Fig. 21 d). On the other hand, scenarios involving the introduction of heat pumps and the combination with storage systems, despite higher CAPEX, they ensure significantly greater amounts of avoided CO_2 emissions, and thus have a lower CAAC impact.

5. Discussion

The objective of this study is to illustrate the low effectiveness of a photovoltaic capacity based on the maximum requirement of an energy district, as common in recent literature.

The aim of the work of Neziric et al. [53] was to assess the feasibility of transforming the Sjeverni logor university campus in Mostar into a positive energy district (PED). This involves combining several buildings into a single energy network to produce more energy than is consumed. Installing solar panels on the campus roofs could generate approximately 750 MWh of electricity annually. The proposed energy generation would exceed the annual energy consumption of the campus buildings, which is estimated at 455 MWh. This would create a positive energy balance, with an estimated surplus of approximately 295 MWh that could be fed into the local power grid. As a result, the surrounding community would benefit from an increased supply of renewable energy.

The study of Frusescu and Minciuc [54] analyses the energy demand of an urban heating district in Bucharest, Romania, and proposes solutions to integrate solar energy into the heating system. The simulation software TRNSYS models the operation of solar thermal and photovoltaic-thermal systems based on energy consumption data. The panels can produce 50 % of their capacity from PT source and 50 % from PVT, 75 % from PT source and 25 % from PVT, 90 % from PT source and 10 % from PVT, or use only 100 % PT or 100 % PVT panel solutions. The maximum useful thermal power obtained from the panels is reached around noon, with a value of 1018 kW and an electrical power of 165 kW. The temperature of the thermal medium outside the collector varies linearly with the power obtained. The maximum temperature for the solar thermal panel is 84.2 °C, while for the PVT it is 75.5 °C.

The article of Tan et al. [55] focuses on analysing the energy consumption of the Zhongjian Building in Lanzhou New District. A photovoltaic system with energy storage is then designed based on the information gathered on the energy consumption and the specific situation of the building. The capacity of the system is configured according to these considerations. To verify the effectiveness of the designed system, simulations are carried out using the PVsyst software. The simulations confirm that the proposed system is capable of generating more than 200 kWh per day, proving its reliability. Finally, the paper analyses the economic and environmental benefits of the system. It concludes that the proposed system offers significant energy savings and reduction of greenhouse gas emissions, that for the CO_2 amounts to 59.08 tons.

[70] investigates the optimal sizing of photovoltaic systems for maximizing self-consumption (SC) and self-sufficiency (SS) while ensuring economic viability through net present value (NPV) assessments. The research is conducted in the context of a subway station in Bucharest, Romania, and utilizes Mixed Integer Linear Programming (MILP) for optimization. The study addresses the integration of PV systems into urban infrastructures, focusing on enhancing SC and SS to reduce dependency on the power grid. Different configurations are examined to determine the balance between SC, SS, and NPV. Integrated approach to optimizing the sizing of photovoltaic (PV) plants specifically for a metropolitan subway station, focusing on maximizing both self-consumption (SC) and self-sufficiency (SS) while also ensuring economic viability through net present value (NPV) calculations, represents the novelty aspect. The results indicate that a properly sized system can achieve significant reductions in grid energy consumption while being economically viable. For the subway station model, the implementation of an optimal PV system could reduce the yearly energy bill by 25 %, signifying a substantial financial saving.

By sizing the photovoltaic system to a higher electricity requirement, which may be the maximum daily, there is a reduction in self-consumption, while the f_{ss} remains virtually unchanged, with higher values for the case with 100 % PV.

The paper approaches the study of the plant system from a macroscopic point of view, refraining from going into the details of application-type problems in depth. Therefore, in the various analyses, Energy, Economic and Environmental some factors have not been taken into account or have been simplified. Therefore, on the one hand, an integration of the analysis is possible for a better evaluation of the scenarios, not that of their feasibility, on the other hand, it is still considered necessary to remain as independent as possible in the evaluations from the specifics of the case.

First of all, it is emphasized that the plant layout of the proposed systems has not been defined. The system is designed for the production of heating, cooling and domestic hot water, particularly in the scenarios involving the replacement of NGB with HP, through the definition of the functional scheme of the system it is possible, for example, to integrate the evaluations with the distribution of loads on the different machines, thus evaluating their transients, such as inrush currents at start-up, as well as defrost cycles, leading to a lowering of COP by as much as 15 % [71]. A further modifier of performance lies in demand-dependent system biasing logics, as well as priority logics on different uses.

In the simulations, distribution and delivery losses were evaluated only through an overall coefficient of 0.97, without considering additional details related to their length, laying and material. While control system and plant zoning were not evaluated. The inclusion of these factors can lead to a significant variation in consumption, as much as 20 percent [72].

From the point of view of electrical output of the PV array this is influenced by installation, shading, azimuth, and tilt. In this case, all panels oriented south and tilted at 35° were considered. More detail of the panel arrangement along the building may bring small variations and considerations regarding the results. Just as the series and parallel configuration of panels and strings and the subdivision of the field can go a long way toward changing the overall productivity of the field [73, 74].

For the different components (PV, HP and TES) we chose models with average efficiency, not to go into the specifics of the individual machines. This implies a generalization of the results, but at the same time less precision. As a further analysis, a sensitivity analysis with different types for the different components can be carried out, however, the objective is to generalize the results with respect to the manufacturer or specific model.

From the economic point of view, no account was taken of the distribution of expenses and consumption on the various apartment buildings, as well as the costs related to the construction of the various plants studied, the mode of energy transit with the network, and the use of any tax incentives. In addition to the above, the natural decay of the performance of the plant over time and the cost of replacing the various components, and other additional charges to ordinary maintenance (considered) lead to changes in the total cost of the plant.

Finally, further considerations that may be made to take account of the real feasibility of the plants concern considerations of a not directly energy-related but of significant practical importance, such as the availability of space and logistics for the installation of all components, as well as acoustic type analysis and compliance with the acoustic terms of law.

The definition of the spaces destined to the new technical power

plants leads however to a variation of the results, is for the economic analysis, involving them a cost, but also energetic going these to influence the length and the distance of the distribution (thermal and electrical) means the number and auxiliary components necessary for the proper operation of the system, such as circulation pumps and pressure calibration valves.

The choice to keep to a non-descript level is in line with the use of the archetype. A more detailed and concrete study of the plant and its components, while maintaining a generalization of the results will be the subject of future studies. A more detailed analysis cannot ignore the macro-scale analysis presented.

6. Conclusions

The development of energy community scenarios can have a significant impact on the energy transition towards renewable energy sources. The integration of technologies such as photovoltaic modules, heat pumps and thermal storage can increase the self-consumption of renewable energy and reduce CO_2 emissions.

The development of energy community scenarios can have a significant impact on the energy transition towards renewable energy sources. The integration of technologies such as photovoltaic modules, heat pumps and thermal storage can increase the self-consumption of renewable energy and reduce CO_2 emissions.

Si parte dalla valutazione di Electrical energy consumption passando all'energia elettrica come vettore energetico e la produzione del PV.

Integration with renewable sources such as PV must be functional to release from the grid, enhancing self-consumption, reducing imported electricity and containing production exportation. In the custom PV plants are designed according to the maximum energy demand, but this is not a guarantee of the best results in terms of self-consumption.

This study aims to provide baseline indications for the project of photovoltaic system in support of energy communities developed on existing neighborhoods. These guidelines, avoiding oversizing, aim to maximize self-consumption depending on the degree of intervention on the ACS heating/cooling system: maintaining the status quo of a system powered by NGB; in the case of a more substantial redevelopment by also acting on heat generators, moving to electricity as an energy carrier thus increasing energy efficiency; introducing thermal storages, technology under development which can be further deepened and optimized.

To conduct these analyses, a useful tool is provided by the creation of an archetype of the neighborhood being studied. In this case it was decided to focus on linear residential buildings constructed in the post-war period, widespread in the Italian stock. The first step was the evaluation of electric energy consumption of the building stock, based on the data measured at Tor Bella Monaca, and the estimate of the production of PV, in the case of plant sized to meet the total or half of electric demand. The analysis of different sizing combinations of photovoltaic systems revealed that simulating a photovoltaic system sized at 50 % of the total energy demand can lead to a high self-consumption of energy compared to the installation of higher electrical power, but also to a reduction of energy fed into the grid. This implies that greater electrification of consumption within an energy community which relies on photovoltaic energy, can increase self-consumption. A further increase in energy self-consumption was demonstrated to result from the application of a thermal storage.

The size of the photovoltaic systems and the integration of other technologies were carefully evaluated to reduce CO_2 emissions. Investment effectiveness was assessed through annual costs (ACs), where CAPEX varies from €357,630 to €1,155,238 over 25 years. Optimal ACs-PES results are for scenarios with maximum plant capacity, while halved PV scenarios require low annual costs for balanced primary energy savings.

Since the analysis was focused on the photovoltaic system and, at the user level, on the macroscopic area of a district, HP were assumed standard, while a sensitivity analysis was carried out for the storage system. The results obtained will constitute the basis for detailed analysis on the PV system, here seen only in two sizes to evaluate the immediate effects of its reduction in extension, and on the issue of the dimensioning of the generator. Electric storage inclusion will be also considered. The archetype of energy community, here preliminary characterized, can be further developed to meet the needs of a real application, by including different types and uses of buildings, currently restricted to linear residential housing.

CRediT authorship contribution statement

Andrea Vallati: Writing – review & editing, Supervision, Project administration, Methodology, Formal analysis, Conceptualization. **Gianluigi Lo Basso:** Supervision, Methodology, Investigation, Conceptualization. **Francesco Muzi:** Writing – review & editing, Writing – original draft, Visualization, Validation, Investigation, Data curation. **Costanza Vittoria Fiorini:** Writing – review & editing, Writing – original draft, Investigation, Formal analysis, Data curation. **Lorenzo Mario Pastore:** Methodology, Formal analysis, Conceptualization. **Miriam Di Matteo:** Writing – review & editing, Writing – original draft, Visualization, Software, Investigation, Data curation.

Declaration of competing interest

The authors declare that they have no known competing financial interests or personal relationships that could have appeared to influence the work reported in this paper.

Data availability

Data will be made available on request.

Acknowledgments

The work was funded by the European Union-Next Generation EU under the PNRR (National Recovery and Resilience Plan – NEST "Network 4 Energy Sustainable Transition" – PE2 NEST Spoke 8 – B53C22004070006).

References

[1] EEA. DIRECTIVE (EU) 2018/2001 OF THE EUROPEAN PARLIAMENT AND OF THE COUNCIL of 11 December 2018 on the promotion of the use of energy from renewable sources. Off J Eur Union 2018;2018.
[2] Lowitzsch J, Hoicka CE, Van Tulder FJ. Renewable energy communities under the 2019 European Clean Energy Package – governance model for the energy clusters of the future. Renew Sustain Energy Rev 2021;122:109489. https://doi.org/10.1016/j.rser.2019.109489.
[3] Cumo F, Maurelli P, Pennacchia E, Rosa F. Urban renewable energy communities and energy poverty: a proactive approach to energytransition with Sun4All project. IOP Conf Ser Earth Environ Sci 2022;1073:012011.
[4] United Nations, "Sustainable development goals.".
[5] Pastore LM, Lo Basso G, Ricciardi G, De Santoli L. Synergies between Power-to-Heat and Power-to-Gas in renewable energy communities. Renew Energy 2022;198 (August):1383–97.
[6] EEA. "DIRECTIVE (EU) 2019/944 OF THE EUROPEAN PARLIAMENT AND OF THE COUNCIL of 5 June 2019 on common rules for the internal market for electricity and amending Directive 2012/27/EU" off. Off J Eur Union 2019;158.
[7] D.L. 30 December 2019, n. 162. Urgent provisions on extension of legislative deadlines, organization of public administrations, and technological innovation.
[8] L.D. 8 November 2021, n. 199. Implementation of directive (EU) 2018/2001.
[9] Pastore LM, Lo Basso G, Quarta MN. Power-to-gas as an option for improving energy self-consumption in renewable energy communities. Int J Hydrogen Energy 2022;47(69):29604–21.
[10] Koutra S, Becue V, Gallas M, Ioakimidis CS. Towards the development of a net-zero energy district evaluation approach : a review of sustainable approaches and assessment tools. Sustain Cities Soc 2018;39(March):784–800.
[11] Derkenbaeva E, Halleck S, Jan G, Van Leeuwen E. Positive energy districts : mainstreaming energy transition in urban areas. Renew Sustain Energy Rev 2022; 153(September 2021):111782. 2021.
[12] Bartolini A, Carducci F, Boigues Muñoz C, Comodi G. Energy storage and multi energy systems in local energy communities with high renewable energy

penetration. Renew Energy 2020;159:595–609. https://doi.org/10.1016/j.renene.2020.05.131. 2020.
[13] Lund H, Østergaard PA, Connolly D, Ridjan I, Mathiesen BV, Hvelplund F, Thellufsen JZ, Sorknses P. Energy storage and smart energy systems, Int. J. Sustain. Energy Plan. Manag 2016;11:3–14. https://doi.org/10.5278/ijsepm.2016.11.2.
[14] Bloess A, Schill W-P, Zerrahn A. Power-to-heat for renewable energy integration: a review of technologies, modeling approaches, and flexibility potentials. Appl Energy 2018;212:1611–26.
[15] Salpakari J, Mikkola J, Lund PD. Improved flexibility with large-scale variable renewable power in cities through optimal demand side management and power-to heat conversion. Energy Convers Manag 2016;126:649–61.
[16] Sternberg A, Bardow A. Power-to-What? - environmental assessment of energy storage systems. Energy Environ Sci 2015;8:389–400.
[17] Hong J, Johnstone C, Torriti L, Leach J. Discrete demand side control performance under dynamic building simulation: a heat pump application. Renew Energy 2012; 39:85–95. https://doi.org/10.1016/J.RENENE.2011.07.042.
[18] Finck C, Li R, Kramer R, Zeiler W. Quantifying demand flexibility of power-toheat and thermal energy storage in the control of building heating systems. Appl Energy 2018;209:409–25. https://doi.org/10.1016/j.apenergy.2017.11.036.
[19] Hany Abokersh H, Saikia MK, Cabeza LF, Boer D, Vallès M. Flexible heat pump integration to improve sustainable transition toward 4th generation district heating. Energy Convers Manag 2020;225:113379. https://doi.org/10.1016/j.enconman.2020.113379.
[20] Fonseca JD, Commenge JM, Camargo M, Falk L, Gil ID. Multi-criteria optimization for the design and operation of distributed energy systems considering sustainability dimensions. Energy 2021;214:118989. https://doi.org/10.1016/j.energy.2020.118989.
[21] Quarton CJ, Samsatli S. Should we inject hydrogen into gas grids? Practicalities and whole-system value chain optimization. Appl Energy 2020;275. https://doi.org/10.1016/j.apenergy.2020.115172.
[22] Abdon A, Zhang X, Parra D, Patel MK, Bauer C, Worlitschek J. Techno-economic and environmental assessment of stationary electricity storage technologies for different time scales. Energy 2017;139:1173–87.
[23] Walker SB, van Lanen D, Mukherjee U, Fowler M. Greenhouse gas emissions reductions from applications of Power-to-Gas in power generation. Sustain Energy Technol Assess 2017;20:25–32.
[24] Lokar J, Virtic P. The potential for integration of hydrogen for complete energy self-sufficiency in residential buildings with photovoltaic and battery storage systems. Int J Hydrogen Energy 2020;45:34566–78. https://doi.org/10.1016/J.IJHYDENE.2020.04.170.
[25] Li Y, Rezgui Y, Zhu H. District heating and cooling optimization and enhancement – towards integration of renewables, storage and smart grid. Renew Sustain Energy Rev 2017;72:281–94. https://doi.org/10.1016/j.rser.2017.01.061.
[26] Pastore LM, Lo Basso G, Ricciardi G, de Santoli L. Smart energy systems for renewable energy communities: a comparative analysis of power-to-X strategies for improving energy self-consumption. Energy 2023;280:128205. https://doi.org/10.1016/j.energy.2023.128205.
[27] Maldonado JL, Tostado-Véliz M, Hasanien M, Khosravi N, Jurado F. Optimal planning of collective photovoltaic arrays in energy communities through a multi-cut benders' decomposition strategy. Sustain Cities Soc 2024;104:105307. https://doi.org/10.1016/j.scs.2024.105307.
[28] Kamal et al, Kamal M, Ashraf I, Fernandez E. Optimal energy management and capacity planning of renewable integrated rural microgrid. Environ Sci Pollut Control Ser 2023;30:99176–97. https://doi.org/10.1007/s11356-023-28792-3.
[29] Servín-Campuzano E, Monserrat Domínguez-Pérez V, Marín-Mendoza PC, Panales-Pérez A, Fuentes-Cortés LF. The role of storage in energy security performance based on diversification and concentration for distributed energy systems. Renew Energy 2024;229:120704. https://doi.org/10.1016/j.renene.2024.120704.
[30] Rehman H, Reda F, Paiho S, Hasan A. Towards positive energy communities at high latitudes. Energy Convers Manag 2019;196:175–95. https://doi.org/10.1016/j.enconman.2019.06.005.
[31] Gjorgievski VZ, Cundeva S, Georghiou GE. Social arrangements, technical designs and impacts of energy communities: a review. Renew Energy 2021;169:1138–56. https://doi.org/10.1016/j.renene.2021.01.078. ISSN 0960-1481.
[32] Cao S, Hasan A, Sirén K. On-site energy matching indices for buildings with energy conversion, storage and hybrid grid connections. Energy Build 2013;64:423–38. https://doi.org/10.1016/j.enbuild.2013.05.030. ISSN 0378-7788.
[33] Alberg Østergaard P. Reviewing EnergyPLAN simulations and performance indicator applications in EnergyPLAN simulations. Appl Energy 2015;154:921–33. https://doi.org/10.1016/j.apenergy.2015.05.086. ISSN 0306-2619.
[34] Gallego-Castillo C, Heleno M, Victoria M. Self-consumption for energy communities in Spain: a regional analysis under the new legal framework. Energy Pol 2021;150:112144. https://doi.org/10.1016/j.enpol.2021.112144. ISSN 0301-4215.
[35] Wang L, He Y, Wu R. Digitization meets energy transition: shaping the future of environmental sustainability. Energies 2024;17:767. https://doi.org/10.3390/en17040767.
[36] Jradi M, Nielsen EW, Lund M. A comprehensive technical analysis of retrofitting a Danish residential area into a positive energy district. Future Cities and Environment 2023;9(1):18. https://doi.org/10.5334/fce.200.
[37] Weckesser T, Franjo Dominković D, Blomgren EMV, Schledorn A, Madsen H. Renewable Energy Communities: optimal sizing and distribution grid impact of photo-voltaics and battery storage. Appl Energy 2021;301:117408. https://doi.org/10.1016/j.apenergy.2021.117408.
[38] Guedes W, Oliveira C, Soares T, Dias B, Matos. Collective asset sharing mechanisms for PV and BESS in renewable energy communities. IEEE Trans Smart Grid 2023. https://doi.org/10.1109/TSG.2023.3288533.
[39] Berg K, Hernandez-Matheus A, Aragüés-Peñalba M, Bullich-Massagué E, Farahmand H. Load configuration impact on energy community and distribution grid: quantifying costs, emissions and grid exchange. Appl Energy 2024;363: 123060. https://doi.org/10.1016/j.apenergy.2024.123060.
[40] Fina B, Auer H, Friedl W. Profitability of PV sharing in energy communities: use cases for different settlement patterns. Energy 2019;189:116148. https://doi.org/10.1016/j.energy.2019.116148. URL, https://www.sciencedirect.com/science/article/pii/S0360544219318432.
[41] Marrasso E, Martone C, Pallotta G, Roselli C, Sasso M. Assessment of energy systems configurations in mixed-use Positive Energy Districts through novel indicators for energy and environmental analysis. Appl Energy 2024;368:123374. https://doi.org/10.1016/j.apenergy.2024.123374.
[42] Palacios-Ferrer JA, Rey-Martínez FJ, Repenning-Bzdigian CA, Rey-Hernández JM. Unveiling key factors shaping energy storage strategies for sustainable energy communities. Buildings 2024;14(5):1466. https://doi.org/10.3390/buildings14051466.
[43] Lin CC, Wu YF, Liu WY. Optimal sharing energy of a complex of houses through energy trading in the Internet of energy. Energy 2021;220:119613. https://doi.org/10.1016/j.energy.2020.119613.
[44] Long C, Wu J, Zhou Y, Jenkins N. Aggregated battery control for peer-to-peer energy sharing in a community Microgrid with PV battery systems. Energy Proc 2018;145:522–7. https://doi.org/10.1016/j.egypro.2018.04.076.
[45] Cosic A, Stadler M, Mansoor M, Zellinger M. Mixed-integer linear programming based optimization strategies for renewable energy communities. Energy 2021; 237:121559. https://doi.org/10.1016/j.energy.2021.121559.
[46] Tan M, Li Z, Su Y, Ren Y, Wang L, Wang R. Dual time-scale robust optimization for energy management of distributed energy community considering source-load uncertainty. Renew Energy 2024;226:120435. https://doi.org/10.1016/j.renene.2024.120435.
[47] Lin XJ, Zhang N, Mao YH, Chen JY, Tian XT, Zhong W. A review of the transformation from urban centralized heating system to integrated energy system in smart city. Appl Therm Eng 2024;240:122272. https://doi.org/10.1016/j.applthermaleng.2023.122272.
[48] Happle G, Fonseca JA, Schlueter A. A review on occupant behavior in urban building energy models. Energy Build 2018;174:276–92. https://doi.org/10.1016/j.enbuild.2018.06.030. ISSN 0378-7788.
[49] Spoladore A, Borelli D, Devi F, Mora F, Schenone C. Model for forecasting residential heat demand based on natural gas consumption and energy performance indicators. Appl Energy 2016;182:488–99. https://doi.org/10.1016/j.apenergy.2016.08.122.
[50] Sood D, Alhindawi I, Ali U, McGrath JA, Byrne MA, Finn D, O'Donnell J. Simulation-based evaluation of occupancy on energy consumption of multi-scale residential building archetypes. J Build Eng 2023;75:106872. https://doi.org/10.1016/j.jobe.2023.106872.
[51] Ferrando M, Ferroni S, Pelle M, Tatti A, Erba S, Shi XF. UBEM's archetypes improvement via data-driven occupant-related schedules randomly distributed and their impact assessment. Sustain Cities Soc 2022;87:104164. https://doi.org/10.1016/j.scs.2022.104164.
[52] Kapalo P, Sulewska M, Adamski M. Examining the interdependence of the various parameters of indoor air, 100 LNCE; 2021. p. 150–7. https://doi.org/10.1007/978-3-030-57340-9_19.
[53] Nezirić E, Špago D, Šarić M, Šunje E, Beća M. University campus as a positive energy district – a case study. In: Ademović N, Kevrić J, Akšamija Z, editors. Advanced technologies, systems, and applications VIII. IAT 2023. Lecture notes in networks and systems, vol. 644. Cham: Springer; 2023. https://doi.org/10.1007/978-3-031-43056-5_44.
[54] Frusescu DC, Minciuc E. A case study about the integration of solar energy solutions in district heating in bucharest, Romania. In: 2023 11th international conference on ENERGY and ENVIRONMENT (CIEM); 2023. p. 1–5. https://doi.org/10.1109/CIEM58573.2023.10349767. Bucharest, Romania.
[55] Tan C, Zhen X, Zhang X, Li S, Wu W, Jiao R. Design of net zero energy building photovoltaic power generation and energy storage system in Lanzhou. In: 2023 7th international conference on smart grid and smart cities (ICSGSC); 2023. p. 501–6. https://doi.org/10.1109/ICSGSC59580.2023.10319183. Lanzhou, China.
[56] Cumo F, Rosa F, Nardecchia F, Agostinelli S. Transforming a historic public office building in the centre of Rome into nZEB: limits and potentials. Energies 2022;15: 697.
[57] Dondi L, Fontanella E, Lepratto F, Morganti M. Ground Level-scape mass-housing adaptive design strategies in Italy. Babel Inte. Barcellona: ListLab 2022.
[58] Ferrando M, Causone F, Hong T, Chen Y. Urban building energy modeling (UBEM) tools: a state-of-the-art review of bottom-up physics-based approaches. Sustain Cities Soc 2020;62.
[59] Reinhart CF, Dogan T, Jakubiec JA, Rakha T. Umi – an urban simulation environment for building energy use , daylighting and walkability energy use , daylighting and walkability. In: 13th conference of international building performance simulation association. France: Chambéry; August . no. August.
[60] Vallati, et al. Building archetype characterization for mass-housing energy efficiency through a UBEM approach. In: Proceeding in conference CISBAT; 2023. paper accepted.
[61] TABULA web tool. https://webtool.building-typology.eu/#bm. [Accessed 10 June 2023].
[62] Lloyd C. Spatial data analysis: an introduction for GIS users. Oxford university press; 2010.

[63] Schneider C, Koltsova A, Schmitt G, Strasse WP. Components for parametric urban design in grasshopper . From street network to building geometry. Building 2010: 68–75. no. January.
[64] EN 16247:2022. Energy Audits.
[65] Martínez-Lera S, Ballester J, Martínez-Lera J. Analysis and sizing of thermal energy storage in combined heating, cooling and power plants for buildings. Appl Energy 2013;106:127–42. https://doi.org/10.1016/j.apenergy.2013.01.074.
[66] Patteeuw D, Helsen L. Combined design and control optimization of residential heating systems in a smart-grid context. Energy Build 2016;133:640–57. https://doi.org/10.1016/j.enbuild.2016.09.030. ISSN 0378-7788.
[67] Zhang Z, Gang W, Zhang Y, Yuan J. Performance analysis of zero-emission integrated energy system for low-density residential building clusters. Renew Energy 2023;219(Part 1):119481. https://doi.org/10.1016/j.renene.2023.119481. ISSN 0960-1481.
[68] Regional Council Resolution of 14/04/2023, n. 101, "Tariff of prices for public construction and plant engineering of Lazio Region - edition 2023".
[69] https://www.arera.it/it/dati/eep35.htm. [Accessed 2 November 2023].
[70] Simoiu MS, Fagarasan I, Ploix S, Calofir V. Optimising the self-consumption and self-sufficiency: a novel approach for adequately sizing a photovoltaic plant with application to a metropolitan station. J Clean Prod 2021;327:129399. https://doi.org/10.1016/j.jclepro.2021.129399.
[71] Roccatello E, Prada A, Baggio P, Baratieri M. Impact of startup and defrosting on the modeling of hybrid systems in building energy simulations. J Build Eng 2023; 65:105767. https://doi.org/10.1016/j.jobe.2022.105767. ISSN 2352-7102.
[72] Hernández FF, Suárez JMP, Cantalejo JAB, Muriano MCG. Impact of zoning heating and air conditioning control systems in users comfort and energy efficiency in residential buildings. Energy Convers Manag 2022;267:115954. https://doi.org/10.1016/j.enconman.2022.115954. ISSN 0196-8904.
[73] Lappalainen K, Valkealahti S. Effects of PV array layout, electrical configuration and geographic orientation on mismatch losses caused by moving clouds. Sol Energy 2017;144:548–55. https://doi.org/10.1016/j.solener.2017.01.066. ISSN 0038-092X.
[74] Zhong Q, Tong D. Spatial layout optimization for solar photovoltaic (PV) panel installation. Renew Energy 2020;150:1–11. https://doi.org/10.1016/j.renene.2019.12.099. ISSN 0960-1481.